

Calcium Isotopic Variations Produced by Biological, Kinetic, Radiogenic and Nucleosynthetic Processes

Donald J. DePaolo

*Department of Earth and Planetary Science
University of California
Berkeley, California 94720, U.S.A.*

*and
Earth Sciences Division
E.O. Lawrence Berkeley National Laboratory
Berkeley, California 94720, U.S.A.*

INTRODUCTION

Study of the isotopic variations of calcium is of interest because Ca is important in geochemical and biochemical processes, and is one of few major cations in rocks and minerals with demonstrated isotopic variability. Calcium is critical to life and a major component of the global geochemical cycles that control climate. Studies to date show that biological processing of calcium produces significant isotopic fractionation (4 to 5‰ variation of the $^{44}\text{Ca}/^{40}\text{Ca}$ ratio has been observed). Calcium isotopic fractionation due to inorganic processing at high (e.g., magmatic) temperatures is small. There are few studies of calcium isotope fractionation behavior for low-temperature inorganic processes. The Ca isotopic variations observed in nature, both biological and inorganic, are mostly attributed to kinetic effects, but this inference cannot be confirmed until equilibrium Ca isotope fractionation is more thoroughly investigated. Evaporation of silicate liquids into vacuum at high temperature is expected to produce kinetic Ca isotopic fractionation, as is diffusion of calcium in silicate liquids and aqueous solutions. The evaporation effects have been observed in meteorite samples. Diffusion effects have been observed in the laboratory but not yet in natural samples. The potential value of Ca isotopic studies has barely been tapped. Improvements in measurement precision would increase the attractiveness of Ca isotopes as a geochemical tool, but such improvements have been slow in coming.

Calcium is composed mainly of the isotope ^{40}Ca , which is a highly stable, doubly magic nuclide (both the number of neutrons and the number of protons represent closed nuclear shells). There are a total of six stable isotopes covering a mass range from 40 to 48. Ca has been studied for isotopic variations in three ways. The major isotope, ^{40}Ca is the primary radioactive decay product of radioactive ^{40}K . About 89.5% of the ^{40}K decays result in the production of ^{40}Ca ; the other 10.5% produce ^{40}Ar and are the basis for the K-Ar and Ar-Ar dating techniques. Rocks and minerals that are both old and rich in potassium can have significant enrichments in ^{40}Ca relative to the other Ca isotopes. The 8-unit spread of isotopic masses also means that there can be significant mass-dependent isotopic fractionation in nature. Consequently there are both radiogenic- and thermodynamically generated Ca isotopic variations in terrestrial materials. In meteorites there is also evidence for isotopic effects reflecting incomplete mixing of materials from different nucleosynthetic sources, combined with processing in the early solar nebula. Some of the mass-dependent variations found in meteorites are quite large (ca. 50‰ variation in the $^{44}\text{Ca}/^{40}\text{Ca}$ ratio).

1529-6466/04/0055-0008\$10.00

CALCIUM ISOTOPE ESSENTIALS

The approximate abundances of the isotopes of calcium are shown in **Table 1**. Russell et al. (1978b) reported the first precise calcium isotope ratio determinations made with modern mass spectrometers. Their measured ratios are shown in Table 1 and constitute the basis for the isotopic abundances and most of the subsequent work described in this article. The Russell et al. (1978b) isotope ratios apply to terrestrial samples that have no significant additions of radiogenic ^{40}Ca beyond the small excesses (ca. 0.01%) expected for average crustal rocks and seawater as discussed below. Niederer and Papanastassiou (1984) and Lee et al. (1977, 1979) used the Russell et al. ratios as the terrestrial reference for assessing non-mass dependent isotopic effects in meteorites. Skulan et al. (1997) used the Russell et al. ratios as a basis for assessing natural mass dependent isotopic variations, and introduced the $\delta^{44}\text{Ca}$ designation (in preference to the $\delta^{40}\text{Ca}$ value used by Russell et al. 1978b). The use of the $^{44}\text{Ca}/^{40}\text{Ca}$ ratio and the $\delta^{44}\text{Ca}$ parameter is more consistent with the notation used for other stable isotope systems, where the heavier isotope is in the numerator and hence higher numbers for both the isotope ratio and the delta value represent relative enrichment of heavy isotopes.

Analysis methods and issues for radiogenic ^{40}Ca

Measurement of radiogenic ^{40}Ca enrichments is mainly done using thermal ionization mass spectrometry (TIMS). The procedures are analogous to those used for other radiogenic isotope measurements. Mass discrimination in the spectrometer must be corrected for using a natural isotope ratio that is not affected by radioactive decay. Because the amount of isotopic discrimination is roughly proportional to the mass difference between isotopes, it makes most sense to choose either the isotope ratio $^{40}\text{Ca}/^{42}\text{Ca}$ or $^{40}\text{Ca}/^{44}\text{Ca}$ to monitor radiogenic enrichments of ^{40}Ca . To measure the mass discrimination it can be advantageous to use an isotope ratio that encompasses a large mass difference between isotopes (such as $^{48}\text{Ca}/^{42}\text{Ca}$ or $^{48}\text{Ca}/^{44}\text{Ca}$). However, there are other considerations that make these ratios unattractive for this purpose. The accuracy of the mass discrimination correction depends on the precision with which the isotope ratio can be measured, which is poorer for lower abundance isotopes. Hence ^{48}Ca is a poor choice, and the combination of ^{48}Ca and ^{42}Ca is particularly unattractive. Also, because the mass discrimination is mass dependent as discussed below, it is advantageous to use an isotope ratio that is similar in average mass to that of the target isotope ratio being measured.

The result of the various considerations is that it is generally best to use either the $^{40}\text{Ca}/^{42}\text{Ca}$ or $^{40}\text{Ca}/^{44}\text{Ca}$ ratios to monitor the radiogenic enrichments of ^{40}Ca , and to use $^{42}\text{Ca}/^{44}\text{Ca}$ to measure mass discrimination. Marshall and DePaolo (1982) chose to use $^{40}\text{Ca}/^{42}\text{Ca}$ as the target ratio and to use $^{42}\text{Ca}/^{44}\text{Ca}$ for the mass discrimination correction. They found that when using the value of $^{42}\text{Ca}/^{44}\text{Ca} = 0.31221$ reported by Russell et al. (1978b) for the mass discrimination correction, the initial solar system value of $^{40}\text{Ca}/^{42}\text{Ca}$ is 151.016 ± 0.008 .

Precise measurement of Ca isotope ratios is challenging because the range of isotopic abundances is large. The value of the ratio $^{40}\text{Ca}/^{42}\text{Ca}$ of ca. 150 means that achieving a typical strong beam intensity of 5×10^{-11} amp for the $^{40}\text{Ca}^+$ ion beam, leaves the $^{42}\text{Ca}^+$ ion beam at an intensity of 3.3×10^{-13} amp. At these levels, counting statistics are a limitation on the measurement precision. Marshall and DePaolo (1982, 1989) used a single collector TIMS instrument to make their measurements, with one-second integration of the $^{40}\text{Ca}^+$ beam and four-second integration of the $^{42}\text{Ca}^+$ beam. At the ion beam intensities quoted above, this yields 3.1×10^8 $^{40}\text{Ca}^+$ ions per measurement and 8.4×10^6 $^{42}\text{Ca}^+$ ions per measurement. Ignoring any complications from background and electronic noise, this means that the accuracy of a single ratio measurement as determined by counting statistics is approximately the uncertainty associated with the measurement of ^{42}Ca , which is about $\pm(8.4 \times 10^6)^{-1/2} \approx \pm 0.3\%$. The theoretical accuracy of the ratio after correction for mass discrimination includes the

uncertainty on the $^{42}\text{Ca}/^{44}\text{Ca}$ measurement, which is about $\pm 0.5\%$, so the overall limit imposed by counting statistics is about 0.6% at the 1σ level. By making ca. 200 measurements, this uncertainty can theoretically be reduced to about $\pm 0.1\%$ (2σ , or about 95% confidence limits) if there are no other sources of noise in the data. In practice, the precision that is achieved with the quoted beam intensities is about ± 0.2 to 0.3% . Although one might think it possible to improve the measurement by integrating the ion beams longer, this does not work for single collector measurements because it increases the amount of time between measurements of the reference isotope, and hence degrades the corrections for the changing beam intensity with time. Counting statistics can also theoretically be greatly improved by use of a multicollector mass spectrometer, where all of the isotopes can be collected at the same time. However, in practice it has been found that while multicollection does in fact improve the precision of individual measurements, there is unaccountable drift that worsens the reproducibility between mass spectrometer runs (e.g., Heuser et al. 2002). Russell et al. (1977, 1978a,b) and Marshall and DePaolo (1982, 1989) achieved a ca. 50% improvement in measurement precision by increasing the beam intensities by $10\times$ relative to those quoted above (i.e., $^{40}\text{Ca}^+$ beam intensity of 4×10^{-10} Amp. Hence the best that has so far been done is a reproducibility of about $\pm 0.15\%$, or ± 1.5 units of ϵ_{Ca} at the 2σ level.

Analysis methods and issues for mass dependent Ca isotope fractionation

The limitations discussed above also apply approximately to measurements of mass dependent Ca isotope effects. The additional problem is to separate mass dependent fractionation in nature from mass dependent fractionation in the mass spectrometer. The maximum observed natural fractionation is about $\pm 0.1\%$ per mass unit, whereas instrumental fractionation is about $\pm 0.5\%$ per mass unit (for TIMS and much larger for ICPMS). The separation is accomplished with the use of a double spike (Russell et al. 1978b). The approach is illustrated here using the methods of Skulan et al. (1997), but other researchers have used slightly different algorithms and double spike isotopes (Zhu and MacDougall 1998; Heuser et al. 2002; Schmitt et al. 2003a).

Once geological samples are dissolved, a mixed ^{42}Ca – ^{48}Ca tracer is added to the sample ($^{42}\text{Ca}/^{48}\text{Ca} \approx 1$). The isotopic abundances in the mixed sample-tracer solution are illustrated in **Figure 1**. When the mixed solution has roughly equal amounts of the isotopes ^{42}Ca , ^{44}Ca , and ^{48}Ca , then a near-optimal situation is achieved with regard to the corrections for the presence of the tracer (cf. Johnson and Beard 1999 for a detailed analysis of spike-sample ratios). The dissolved sample-tracer mixture is then loaded onto a cation exchange column and eluted with 2.5N HCl. This step is needed to separate Ca from other major cations such as Mg, Ti, Fe, Na, K, and Al. The purified Ca is loaded onto Re filaments with tantalum oxide powder for mass spectrometric analysis. It is important to mix the sample and double-spike tracer solution prior to ion exchange separation of Ca because the ion exchange column can introduce substantial mass-dependent isotopic fractionation if the Ca yield of the column is not close to 100% (Russell et al. 1978a).

The mass spectrometric analysis using Ca^+ ions and is carried out (at University of California, Berkeley) on a single-collector mass spectrometer: a modified VG354 design with one large Faraday bucket collector. Ca has been difficult to analyze reliably using a multi-collector mass spectrometer due to unspecified problems that cause poor reproducibility. Multi-collector runs typically result in excellent internal precision ($\approx 0.05\%$), but poor external precision (reproducibility of standards and repeat runs of samples can be as large as $\pm 0.5\%$), apparently because the measurements are affected by subtle differences in focusing from sample to sample (cf. Heuser et al. 2002). The single collector method has the disadvantage of requiring a very stable ion beam and long analysis times (several hours per sample), but the advantage of needing much less calibration, relative to the multi-collection method. There is an expectation that certain design improvements to the latest generation multi-collector

instruments will make them more attractive for Ca isotope measurements. Fletcher et al. (1997b) and Heuser et al. (2002) report multi-collector TIMS measurements but do not report a large improvement in reproducibility. Halicz et al. (2000) report multi-collector ICPMS measurements with reproducibility similar to that achieved with other methods.

Normally it is possible to obtain stable $^{40}\text{Ca}^+$ ion beams with intensities up to about 10^{-10} amp. This intensity requires that about 3–5 μg of Ca be loaded onto the mass spectrometer filament. The amount of Ca needed for analysis is not generally a problem, because Ca is a major constituent of bone and shell material, and is present in natural waters in relatively high concentration as well. The intensity of the $^{40}\text{Ca}^+$ ion beam is adjusted so that it is between 6 and 9×10^{-11} amp. Beam intensity is normally kept within a narrow range for all measurements because large ion beams can produce a non-linear response of the amplifier feedback resistor. If the beam intensity is kept within a small range, the effect of any non-linearity on measured isotope ratios is minimized when samples and standards measured with the same instrument are compared. The large $^{40}\text{Ca}^+$ peak is integrated for one second whereas five second integrations are used on the smaller peaks $^{42}\text{Ca}^+$, $^{44}\text{Ca}^+$ and $^{48}\text{Ca}^+$, which are about 40 times smaller than $^{40}\text{Ca}^+$. For the smaller peaks this results in the counting of 5×10^7 ions per measurement, and for 200 measurements per sample per isotope, with the corrections involved, yields an analytical uncertainty of 0.1 to 0.2‰ at the 2σ level.

Using the three measured ratios, $^{42}\text{Ca}/^{40}\text{Ca}$, $^{44}\text{Ca}/^{40}\text{Ca}$ and $^{48}\text{Ca}/^{40}\text{Ca}$, three unknowns can be solved for: the tracer/sample ratio, the mass discrimination, and the sample $^{44}\text{Ca}/^{40}\text{Ca}$ ratio (see also Johnson and Beard 1999; Heuser et al. 2002). Solution of the equations is done iteratively. It is assumed that the isotopic composition of the ^{42}Ca – ^{48}Ca tracer is known perfectly, based on a separate measurement of the pure spike solution. Initially it is also assumed that the sample calcium has a “normal” Ca isotopic composition (equivalent to the isotope ratios listed in Table 1). The $^{42}\text{Ca}/^{48}\text{Ca}$ ratio of the tracer is determined based on the results of the mass spectrometry on the tracer-sample mixture, by calculating the effect of removing the sample Ca. This yields a $^{42}\text{Ca}/^{48}\text{Ca}$ ratio for the tracer, which is in general different from that previously determined for the tracer. This difference is attributed to mass discrimination in the spectrometer ion source and is used to calculate a first approximation to the parameter “ p ” which describes the instrumental mass discrimination (see below). The first-approximation “ p ” is used to correct the *measured* isotope ratios for mass discrimination, and then a first-approximation tracer/sample ratio and a first-approximation sample $^{44}\text{Ca}/^{40}\text{Ca}$ ratio are calculated with standard spike-subtraction equations. This first-approximation sample $^{44}\text{Ca}/^{40}\text{Ca}$ ratio is in general different from the standard ratio, as a result of natural mass fractionation. Using the first approximation sample $^{44}\text{Ca}/^{40}\text{Ca}$ ratio, the $^{42}\text{Ca}/^{40}\text{Ca}$ and $^{48}\text{Ca}/^{40}\text{Ca}$ ratios are corrected for the natural mass fractionation, and these once-corrected sample Ca isotope ratios are then used to determine a second-approximation $^{42}\text{Ca}/^{48}\text{Ca}$ for the tracer, a second approximation “ p ,” and second-approximation values of tracer/sample and sample $^{44}\text{Ca}/^{40}\text{Ca}$. This is continued until “ p ” no longer changes at the level of 1 ppm, which requires 3 to 5 iterations. The measured sample $^{44}\text{Ca}/^{40}\text{Ca}$ ratio is then converted to $\delta^{44}\text{Ca}$ using the relationship shown in Table 1.

The essential nature of the exponential parameterization of instrumental mass discrimination given by Russell et al. (1978b) is represented by the following two equations:

$$\frac{^{44}\text{Ca}}{^{40}\text{Ca}_{\text{frac}}} = \frac{^{44}\text{Ca}}{^{40}\text{Ca}_{\text{unfrac}}} \left(\frac{M_{44}}{M_{40}} \right)^p \quad (1a)$$

$$\frac{^{48}\text{Ca}}{^{44}\text{Ca}_{\text{frac}}} = \frac{^{48}\text{Ca}}{^{44}\text{Ca}_{\text{unfrac}}} \left(\frac{M_{48}}{M_{44}} \right)^p \quad (1b)$$

which gives the relationship between “fractionated” ratios and “unfractionated” ratios for two Ca isotope ratios. The parameters M_n are the exact atomic masses of the isotopes of mass number “ n ,” and p is the discrimination parameter. These two equations show that for the same value of p , the amount of fractionation is greater for $^{44}\text{Ca}/^{40}\text{Ca}$ than it is for $^{48}\text{Ca}/^{44}\text{Ca}$; the discrimination is dependent not on the mass difference, but on the fractional mass difference (mass 44 is about 10% larger than mass 40, but mass 48 is only about 9.1% larger than mass 44). It is assumed that the fractionation of Ca isotopes in the mass spectrometer and the fractionation in nature are described by the same exponential law. If this were not the case it would make little difference to the results, because Ca isotopic fractionation in nature is sufficiently small.

Ca isotope standards and reference materials

The tracer-subtraction procedure adds negligible uncertainty to the measured $^{44}\text{Ca}/^{40}\text{Ca}$ ratios. However, it is in fact essentially impossible to entirely eliminate the effects of instrumental mass discrimination for the measurements of either the ^{42}Ca - ^{48}Ca mixed tracer or for the “standard” Ca isotope ratios. Hence, in the end it is necessary to have a standard material with an agreed-upon value of $\delta^{44}\text{Ca}$. At the time of writing of this article there is no such standard.

The isotope ratios listed in Table 1 are those of a CaF_2 purified salt used as an in-house standard by Russell et al. (1978b). Skulan et al. (1997) used a different purified Ca salt as a standard and showed that the $\delta^{44}\text{Ca}$ values measured for several terrestrial igneous rocks were close to zero on this scale. The Skulan et al. (1997) scale for $\delta^{44}\text{Ca}$ is used here. Zhu and MacDougall (1998) used a standard $^{44}\text{Ca}/^{40}\text{Ca}$ ratio (0.021747) that is 2.5% higher than the Russell et al. (1978b) value. However, they report all of their measured $\delta^{44}\text{Ca}$ values relative to seawater, which has a $\delta^{44}\text{Ca}$ value of +0.9 on the Skulan et al. (1997) scale. Hence the Zhu and MacDougall (1999) $\delta^{44}\text{Ca}$ values discussed here have 0.9 added to them to make them compatible with the Skulan et al. (1997) scale. Nägler et al. (2000) report $\delta^{44}\text{Ca}$ values relative to an in-house fluorite standard. Based on Figure 1 of Gussone et al. (2003), where seawater is plotted with $\delta^{44}\text{Ca} = +0.43$, it can be deduced that the $\delta^{44}\text{Ca}$ value of the fluorite standard used by Nägler et al. (2000) is close to +0.5 on the Skulan et al. (1997) scale. Hence, 0.5 has been added to the $\delta^{44}\text{Ca}$ values reported by Nägler et al. (2000) and Gussone et al. (2003). Schmitt et al. (2003a,b) report values for seawater and refer their measured values to seawater Ca as a standard (i.e., seawater $\delta^{44}\text{Ca} = 0$). Hence, 0.9 has been added to the $\delta^{44}\text{Ca}$ values reported by Schmitt et al.

As shown below, the $\delta^{44}\text{Ca} = 0$ as defined by Skulan et al. (1997) corresponds closely to the isotopic composition of calcium in igneous rocks (Table 2), and hence probably is close to the value for the bulk Earth. It is preferable to define $\delta^{44}\text{Ca} = 0$ as the bulk Earth value rather than that of seawater, because the seawater value is determined by geological processes that can change with time (discussed below), whereas the bulk Earth value represents the bulk of the Ca in the planet and does not change. Seawater also has a small radiogenic enrichment of ^{40}Ca relative to bulk Earth calcium (see discussion below). However, there is not yet a generally accepted rock standard, and there are small variations among volcanic rock samples (Table 2). An appropriate standard is needed, preferably a rock sample with high Ca and low K abundance, and with the mantle $^{40}\text{Ca}/^{42}\text{Ca}$ ratio (i.e., with negligible radiogenic ^{40}Ca). Some authors have measured the NIST calcium carbonate standard SRM915a (Schmitt et al. 2003a,b; Gussone et al. 2003), and that standard could serve to facilitate inter-laboratory comparisons. The results from SRM915a suggest that the adjustments made here to the reported $\delta^{44}\text{Ca}$ values are appropriate and accurate within about $\pm 0.1\text{‰}$.

CALCIUM ISOTOPES IN METEORITES AND LUNAR SAMPLES

The Ca isotope ratios of meteoritic samples are of interest because they can give information on early solar system processes and because meteorites represent the materials from which the Earth accreted and hence relate to the expected values for the bulk Earth. Russell et al. (1978b) made the first measurements of stable Ca isotope variations in meteorites. They found variations of about $\pm 1\%$ for the $^{44}\text{Ca}/^{40}\text{Ca}$ ratio in samples from six different meteorites. Although some of these samples were spiked after having separated the Ca with an ion exchange column and hence may contain artifacts, it is clear from their data that bulk meteorites have some variability in $\delta^{44}\text{Ca}$ and that the average value is quite close to the terrestrial standard. No data on bulk meteorites have been reported since the Russell et al. (1978) measurements, and since their one measurement of an ordinary chondrite had a poor Ca column yield, there exist no reliable measurements that can be used to verify the composition of typical chondritic meteorites.

Russell et al. (1977, 1978b) also measured two Apollo 17 and one Apollo 15 basalt samples and found small variations of $\delta^{44}\text{Ca}$ of ca. $\pm 1\%$, but again also spiked the samples after ion exchange separation so the results need to be verified. Russell et al. (1977) measured calcium obtained by lightly leaching an Apollo 15 soil sample and found it to have $\delta^{44}\text{Ca}$ of $+3.3 \pm 0.4$. This heavy Ca is inferred to be associated with the grain surfaces and result from solar wind sputtering.

Lee et al. (1977, 1979), Niederer and Papanastassiou (1984), Jungck et al. (1984), Ireland et al. (1991) and Russell et al. (1998) reported Ca isotopic measurements on calcium-aluminum rich inclusions (CAI) and calcium-rich aggregates (CA) from the Allende meteorite. Both the CAI and CA show large mass-dependent fractionation effects (**Fig. 2**). The overall range of $\delta^{44}\text{Ca}$ is about 10 times larger than is found in terrestrial materials. The large mass fractionation effects are attributable to non-equilibrium evaporation from liquid or partially molten silicate droplets in the solar nebula. Light isotopes of Ca can be preferentially lost during evaporation into a near-vacuum, leaving residual Ca enriched in heavy isotopes and hence with high $\delta^{44}\text{Ca}$. Condensation of light Ca from a vapor phase can generate solids with low $\delta^{44}\text{Ca}$. Apparently both processes affected the calcium-aluminum rich materials. Similar fractionation effects are found also in Mg isotopes (Lee et al. 1977, 1979) and silicon isotopes (Clayton et al. 1988), although correlations between Ca isotope fractionation effects and Mg isotope fractionation effects are complex (Niederer and Papanastassiou 1984). Experimental studies have simulated the Si and Mg isotopic effects of high temperature evaporation into a low-pressure hydrogen medium similar to the solar nebula (Davis et al. 1990; Richter et al. 2002) and current models for the formation of CAI's involve cycling through the inner, high-temperature part of the nebula (Shu et al. 1996; Davis and MacPherson 1996) and consequently there are ample opportunities for heating and cooling to generate evaporation and recondensation.

The studies by Lee et al. (1977, 1979), Niederer and Papanastassiou (1984), as well those by Jungck et al. (1984), Ireland et al. (1991), Weber et al. (1995) and Russell et al. (1998), report small deviations of the abundances of ^{42}Ca , ^{46}Ca and ^{48}Ca relative to those of terrestrial materials. The most commonly observed deviation from normal terrestrial isotopic abundances is enrichment in ^{48}Ca , which can be quite large (Fig. 2b). These deviations are significant because they provide direct evidence for the existence of certain (in this case neutron-rich) nucleosynthetic environments in stars (cf. Cameron 1979 and references in the other papers listed above).

TERRESTRIAL STUDIES OF RADIOGENIC CALCIUM

The radioactive, naturally occurring isotope of potassium— ^{40}K —decays by β^- emission

to ^{40}Ca . The accepted value for the total decay constant of ^{40}K is $5.543 \times 10^{-10} \text{ yr}^{-1}$, which corresponds to a half-life of 1.25 billion years (Steiger and Jager 1977). As a consequence of radioactive decay, the abundance of ^{40}Ca increases with time in any substance that contains potassium, and this increase is independent of any mass-dependent isotopic fractionation of Ca isotopes. The equation describing the increase in ^{40}Ca with time can be written:

$$\frac{{}^{40}\text{Ca}}{n\text{Ca}}(t) = \frac{{}^{40}\text{Ca}}{n\text{Ca}}(t_o) + \frac{{}^{40}\text{K}}{n\text{Ca}}(t) R_{\beta-} \left[e^{\lambda_{40}(t-t_o)} - 1 \right] \quad (2)$$

where n is the mass number of one of the non-radiogenic Ca isotopes, λ_K is the total decay constant of ^{40}K , and $R_{\beta-}$ is the branching ratio (Steiger and Jaeger 1977):

$$R_{\beta-} = \frac{\lambda_{\beta-}}{\lambda_K} = 0.8952$$

To maximize analytical precision and reproducibility, Marshall and DePaolo (1982) chose $n = 42$, and hence report all data in terms of $^{40}\text{Ca}/^{42}\text{Ca}$ ratios normalized to $^{42}\text{Ca}/^{44}\text{Ca} = 0.31221$. This choice allows one to use an isotope ratio spanning two mass units ($^{42}\text{Ca}/^{44}\text{Ca}$) to make a correction (for instrumental mass discrimination) to another isotope ratio spanning two mass units ($^{40}\text{Ca}/^{42}\text{Ca}$). The only other likely choice is to use $^{40}\text{Ca}/^{44}\text{Ca}$ (i.e., $n = 44$), which spans four mass units and hence would have twice as large a correction for instrumental mass discrimination.

Marshall and DePaolo (1982) demonstrated the use of the K-Ca method for geochronology by dating the Pikes Peak granite, which has also been dated by other methods (Fig. 3). Earlier work on K-Ca geochronology is reported by Inghram et al. (1950), Herzog (1956), Plevaya et al. (1958), and Coleman (1971). The earlier studies did not have the benefit of the more precise isotope ratio measurement techniques offered by automated mass spectrometers and were restricted to studies of minerals like sylvite and lepidolite which have extremely high K/Ca ratios. Baadsgaard (1987) also measured K-Ca ages of evaporite minerals and used them to clarify the prolonged history of diagenesis of the deposits. More recently Nägler and Villa (2000) measured both K-Ar and K-Ca ages on gem quality minerals in an attempt to measure the ^{40}K branching ratio on natural samples. They found that Ar ages are systematically younger by a few to several percent than K-Ca ages and suggest a small revision of the branching ratio based on one of their samples. However, the ultimate conclusion is that Ar loss from natural samples cannot be ruled out and hence any measurement of the branching ratio using geological samples is likely to have too much uncertainty to make one confident about revising the currently accepted value. Marshall et al. (1986) measured both K-Ca and K-Ar ages on Paleozoic authigenic sanidine and found that the K-Ar ages were systematically 8% younger. They interpreted the data to mean that Ar had diffused out of the sanidine, and that the diffusivity of Ar at ca. 20°C was several orders of magnitude higher than would be deduced from high temperature diffusion data. Fletcher et al. (1997a) measured both K-Ca and Rb-Sr ages in muscovites from Archean granitic rocks in Australia and found that the K-Ca dates are in general substantially younger than the Rb-Sr dates, and both are substantially younger than the accepted crystallization age of the rocks. Fletcher et al. (1997a) infer that the diffusivity of Ca in micas is about an order of magnitude greater than Sr in micas.

Because the ^{40}Ca isotopic enrichments in whole rocks are relatively small, Marshall and DePaolo (1982, 1989) used the ϵ_{Ca} value as defined in Table 1, which refers the $^{40}\text{Ca}/^{42}\text{Ca}$ value of rocks to the value expected in the Earth's mantle. Strictly speaking, the $^{40}\text{Ca}/^{42}\text{Ca}$ value of the mantle changes with time. However, taking the approximate value of K/Ca of the mantle to be 0.01, the $^{40}\text{K}/^{42}\text{Ca}$ ratio is about 0.0002, and the total change of $^{40}\text{Ca}/^{42}\text{Ca}$ over the age of the Earth is 0.002 or about 0.12 units of ϵ_{Ca} .

In general, magmas generated by melting of the mantle should have negligible enrichments of ^{40}Ca and hence have ϵ_{Ca} values that are zero within the analytical resolution of about ± 1 . However, granitic magmas that are melted from ancient K-rich crustal rocks can have significant enrichments of ^{40}Ca . The data reported by Marshall and DePaolo (1982, 1989) are shown in **Figure 4**. The highest ϵ_{Ca} values are found in granitic rocks with high K/Ca ratios (Fig. 4a) and with low ϵ_{Nd} values that indicate magma derived from crustal rocks (Fig. 4b). Based on the Sm-Nd model ages of the rocks, which are 1.8 to 3 Ga, the high ϵ_{Nd} values of the Tertiary and Cretaceous granites indicate that the magmas were melted from crustal rocks that had K/Ca ratios of about 0.5 to 2. Such high K/Ca values generally correspond to rocks with SiO_2 contents of about 65%. The Wyomingite lava measured from the Leucite Hills, which has a very high K/Ca ratio, shows very little ^{40}Ca enrichment as is expected for mantle rocks insofar as “enriched mantle” is unlikely to have a K/Ca ratio much higher than about 0.1. An unexpected aspect of the data, which has gone unconfirmed, is the slight enrichment of ^{40}Ca observed for island arc andesites and some low-K, high ϵ_{Nd} granitic rocks from the western Sierra Nevada. This effect would suggest that a large fraction of the calcium in island arc lavas comes from subducted carbonates, seawater-altered oceanic crust, and/or continental sediments. Nelson and McCulloch (1989) also reported a number of analyses of ϵ_{Ca} on mafic igneous rocks including carbonatites, kimberlites, ultrapotassic lavas, and island arc basalts. Some of their samples appear to have slightly elevated ϵ_{Ca} , but their interpretation was that none of the enrichments was clearly outside the analytical uncertainty of ± 1.8 units.

Because of the 1.25 Gyr half-life of ^{40}K , a large amount of the Earth's ^{40}K has decayed over the past 4.55 Gyr. The $^{40}\text{K}/^{39}\text{K}$ ratio was higher by about 12.5 times at the time of formation of the earth relative to the present ratio, and was still enhanced by 4 to 9 times at 2.5 to 4.0 Ga. Consequently, ancient high-K granites can potentially have larger ϵ_{Ca} values if derived from yet older high-K crustal rocks. This aspect of the K-Ca system was employed by Shih et al. (1994) for dating of a ca. 3.6 Ga lunar “granite.” However, the K-Ca age obtained on the granite was lower than the likely crystallization age.

The average age of continental crustal rocks is about 2 Ga. The typical upper crustal rock has K/Ca of 0.9 and the bulk continental crust has a ratio of about 0.35 (Rudnick & Fountain 1995, Taylor and McLennan 1995, Shaw et al. 1986, Condie 1993, Wedepohl 1995). Using these values, the average continental crustal value for ϵ_{Ca} is 0.8 and that for upper continental crust is 2.0. Marshall et al. (1986) measured modern shell material representative of seawater and found it to have an ϵ_{Ca} value of $+1.5 \pm 1.0$ (Fig. 4a). The slight enrichment of ^{40}Ca in seawater is consistent with the estimated crustal ϵ_{Ca} values.

Effects of radiogenic calcium ^{40}Ca on measured $\delta^{44}\text{Ca}$ values

Radiogenic enrichments of ^{40}Ca can be accounted for in the double spike technique simply by changing the reference value of the $^{40}\text{Ca}/^{44}\text{Ca}$ ratio for “unfractionated” calcium (Table 1). Figures 3 and 4a show on the right hand scale the equivalent value of $\delta^{44}\text{Ca}$ that would be deduced from a double spike measurement that did not account for the radiogenic enrichment of ^{40}Ca . The $^{40}\text{Ca}/^{44}\text{Ca}$ values reported by Russell et al. (1978b), which were measured on purified CaF_2 , probably represent continental crustal values and hence include an enrichment of ^{40}Ca of perhaps 0.1 to 0.2% relative to mantle samples and meteorites. This difference is only marginally significant because the typical analytical uncertainty is also about 0.1 to 0.2‰. However, the radiogenic component must be recognized (cf. Zhu and MacDougall 1998) and can be significant if not dominant in some cases. For example, in soils it is often found that biotite weathers faster than other silicate minerals (White et al. 1996; Blum and Erel 1997). Calcium derived from weathering biotite from the Pikes Peak granite (Fig. 3) would appear to have a $\delta^{44}\text{Ca}$ value of -6 , and the Ca from the K-feldspar would have $\delta^{44}\text{Ca}$ of about -4 . The radiogenic component of calcium from potassium minerals could be beneficial for tracing the fate of the calcium from these minerals during weathering and soil formation and

during metamorphism (Marshall 1984). To be rigorous, the measurement of stable isotope fractionation effects should include determinations of the radiogenic ^{40}Ca enrichment as well (Zhu and MacDougall 1998; Schmitt et al. 2003b). In practice this is not necessary for many samples, and in addition the small ^{40}Ca enrichments are typically difficult to resolve. For example, Schmitt et al. (2003b) use seawater as a reference and claim to be able to resolve radiogenic ^{40}Ca effects at the level of about $\pm 0.2\%$. The seawater value of $\delta^{44}\text{Ca}$, 0.15 ± 0.2 , covers most of the observed range in whole rock samples due to radiogenic effects (Fig. 4a).

STUDIES OF TERRESTRIAL CALCIUM STABLE ISOTOPE FRACTIONATION

Igneous and metamorphic rocks and petrogenetic processes

The measurements that are available to assess high temperature fractionation of Ca isotopes in nature do not constitute a representative sampling of crystalline rocks; most of the samples measured are volcanic and are relatively common rock types (Table 2; Fig. 5). There are few or no measurements available for clastic sedimentary rocks, soils, high-K granites, and many other rock types that might be of interest. All of the measured $\delta^{44}\text{Ca}$ values of typical volcanic rocks are between -0.3 and $+0.3$. The mean and standard deviation of the values from the table is -0.11 ± 0.18 . Since virtually all of the samples listed in Table 2 are mantle-derived rocks with no significant involvement of old continental rocks, the $\delta^{44}\text{Ca}$ values do not reflect any radiogenic ^{40}Ca enrichment. Hence the slightly negative average value may in fact be confirmation that the mantle $^{40}\text{Ca}/^{44}\text{Ca}$ ratio is slightly lower than the value for the Skulan et al. (1997) standard. The variation of the $\delta^{44}\text{Ca}$ values is larger than analytical uncertainty, which suggests that there are small variations in igneous rocks that are barely resolvable with current techniques. There are some hints that the $\delta^{44}\text{Ca}$ values may correlate with other isotopic parameters (Fig. 5), but there are too few data to be definitive.

Richter et al. (2003) have shown experimentally that there are physical processes that can fractionate Ca isotopes significantly (Fig. 6). A diffusion couple consisting of basaltic liquid (10.38% CaO) and rhyolitic liquid (0.5% CaO) was allowed to evolve for 12 hours at a temperature of 1450°C . Isotopic effects are generated during multi-component diffusion where Ca (as well as Mg, Fe, etc.) diffuses from the basalt liquid into the rhyolite liquid. The basalt and rhyolite start out with identical $\delta^{44}\text{Ca}$ values of -0.2 . The lighter isotopes of Ca diffuse slightly faster than the heavier isotopes and consequently the basalt becomes enriched in heavy Ca while the rhyolite develops a negative $\delta^{44}\text{Ca}$ value. As shown in the figure, the experiment generates an isotopic contrast of about 6.5% in $\delta^{44}\text{Ca}$ where none existed at the outset. This type of effect has not yet been observed in natural samples, but the experiments confirm that diffusion within silicate melts can fractionate Ca isotopes. Richter et al. (2003) modeled the results and found that the ratios of the diffusivities of the two isotopes is described approximately by:

$$\frac{D_{44}}{D_{40}} = \left(\frac{m_{40}}{m_{44}} \right)^{0.075} \quad (3)$$

where D_{44}/D_{40} is the ratio of the diffusivities of the diffusing species containing ^{44}Ca and ^{40}Ca respectively, and m_{40} and m_{44} are the nuclidic masses of the two calcium isotopes. This result indicates that the masses of the diffusing species are considerably larger than the masses of the individual Ca atoms. Richter et al. (2003) did not comment on the nature of the diffusing species in the silicate liquid. However, it may be noteworthy that, for the ratio of the diffusivities to equal the square root of the mass of the diffusing species, the diffusing species containing ^{40}Ca needs to have a mass of about 278, exactly the mass of the anorthite formula

unit ($^{40}\text{CaAl}_2\text{Si}_2\text{O}_8$). Hence, a model using the anorthite formula unit as the diffusing species would be consistent with the observations. This approach could be useful for estimating the polymer sizes associated with cations in silicate melts.

Biological fractionation through food chains

The observation suggesting that biological processes fractionate Ca isotopes is the systematic lowering of $\delta^{44}\text{Ca}$ values through food chains (Skulan et al. 1997). In both terrestrial and marine environments, carnivores at the end of the food chain have significantly lighter skeletal $\delta^{44}\text{Ca}$ values (Fig. 7). The starting point for the marine systems is seawater, which is about 1‰ higher in $\delta^{44}\text{Ca}$ than average igneous rocks (the reason for this is discussed further below). Organisms that obtain their Ca directly from seawater, such as foraminifera, mollusks, and fishes, have $\delta^{44}\text{Ca}$ values of about +0.5 to −1.0. Seals, which get their Ca from smaller organisms rather than seawater, have an average $\delta^{44}\text{Ca}$ value of about −1.3. Bone from an orca is the lightest material so far measured in a higher marine organism at −2.3. The total difference between orca bone and seawater is 3.2‰. For terrestrial organisms the range of $\delta^{44}\text{Ca}$ is similar to that found in the marine environment, but the $\delta^{44}\text{Ca}$ values are lower. In a small sampling of materials in Northern California and in New York (Skulan 1999; Skulan and DePaolo 1999) it is found that whole soils are close to or slightly higher than rock values for $\delta^{44}\text{Ca}$, plants are about 1‰ lower, horse and deer have bone $\delta^{44}\text{Ca}$ values of about −2 and a cougar has a bone $\delta^{44}\text{Ca}$ value of −3.2. The total range of $\delta^{44}\text{Ca}$ values in the terrestrial environment is also about 3.5‰.

The Ca isotope data from food chains indicates that the Ca fixed in mineral matter in organisms is typically lighter than the Ca available to them from their surroundings or through their diets. In succeeding levels of a food chain the $\delta^{44}\text{Ca}$ values decrease by about 1 unit per level. Terrestrial animals at analogous levels of the food chain tend to have $\delta^{44}\text{Ca}$ values that are about 1 unit lower than their marine counterparts. A recent report by Clementz et al. (2003) confirms the systematic relationship between $\delta^{44}\text{Ca}$ and trophic level in marine organisms, and suggests that the relationship is preserved in 15 million year old bone specimens as well. Skulan (1999) also analyzed a large number of fossil bone and shell samples and suggests that Ca isotopes can be used for paleodiet reconstruction.

Model for Ca isotope fractionation in vertebrates

In an effort to further elucidate the nature of Ca isotope fractionation in animals, Skulan and DePaolo (1999) studied tissues from living and recently deceased (naturally) organisms. For the four animals studied, it was found that bone calcium typically has $\delta^{44}\text{Ca}$ that is 1.3‰ lower than the value in the dietary calcium (Fig. 8). The soft tissue calcium, however, is quite variable, and has values closer to that of the dietary calcium. Skulan and DePaolo (1999) concluded that the primary source of Ca isotope fractionation was in the formation of bone, and that the $\delta^{44}\text{Ca}$ values of soft tissue were variable in time and dependent on the immediate status of the Ca balance in the organisms.

The model proposed for understanding the Ca balance, and both the soft tissue and bone $\delta^{44}\text{Ca}$ values (Fig. 9) suggests that the isotopic values are dependent on the ratio of the available Ca coming from dietary intake, and the rate of bone growth and/or bone loss. The assumption is that exchange of Ca between different soft tissues involves negligible isotopic fractionation. Fractionation occurs only when Ca is fixed into bone, and the fractionation factor is about −1.5‰ (Fig. 9a). If the dietary supply of Ca (V_d) is much larger than the rate of Ca use by bone growth (V_b), then bone should have $\delta^{44}\text{Ca}$ about 1.5 units lower than the dietary Ca, and the average $\delta^{44}\text{Ca}$ value of soft tissue is close to that of the dietary source (Fig. 9b). However, if a large fraction of the dietary supply is being used to produce new bone (i.e., $V_b/V_d \approx 1$), the bone $\delta^{44}\text{Ca}$ values will be closer to that of the dietary supply, and the soft tissue values will be higher than those of the diet. If there is a significant amount of bone loss by

comparison with the dietary Ca supply ($V_i/V_d \geq 1$), then the low- $\delta^{44}\text{Ca}$ calcium coming from dissolving bone will make the soft tissue $\delta^{44}\text{Ca}$ values low (Fig. 9c).

The net result, according to the model, is that under circumstances that might be considered typical of healthy juvenile organisms—substantial bone growth but with ample dietary Ca supply—typical bone material is slightly less than 1.5‰ lower in $\delta^{44}\text{Ca}$ than dietary calcium. In healthy adults, where new bone growth is balanced by bone loss (remodeling), there would be little tendency for the average bone $\delta^{44}\text{Ca}$ values to change. If there is a shortage of dietary Ca while new bone is being made in juveniles, then the bone $\delta^{44}\text{Ca}$ values will be closer to the dietary values. If there is major bone loss in adults, then soft tissue (and remodeled bone) $\delta^{44}\text{Ca}$ values will be exceptionally low (Fig. 9c). The bone $\delta^{44}\text{Ca}$ values reflect conditions integrated over the residence time of bone Ca, which is many years. Soft tissue $\delta^{44}\text{Ca}$ values, however, may reflect the conditions of the Ca balance within hours or days of the sampling time. For example, the low $\delta^{44}\text{Ca}$ value of muscle Ca in the fur seal, which was found dead, suggests that it had a dietary Ca deficiency for at least several days before it died.

Ca isotope fractionation in marine shelled organisms

The calcium carbonate shells of marine microfauna are a large repository of terrestrial calcium and constitute a potential record of changes in the cycling of calcium at and near the earth's surface (Zhu and MacDougall 1998; De La Rocha and DePaolo 2000; Schmitt et al. 2003a,b). To understand the record held in deep sea carbonate sediments, it is necessary to document any Ca isotopic fractionation that occurs between dissolved seawater Ca and carbonate shell material.

Skulan et al. (1997) reported analyses of marine carbonate sediments of various ages and analyses of foraminifera tests and other marine organisms. They concluded that typical marine shell material had $\delta^{44}\text{Ca}$ values that are about 1‰ lower than seawater Ca, and that there might be a small temperature dependence of about 0.02 per degree. Zhu and MacDougall (1998) reported measurements of foraminifera that indicate that the carbonate $\delta^{44}\text{Ca}$ values are 0.56 to 1.45‰ lower than those of seawater, and suggested that there was a temperature dependence to the fractionation within individual species, at the level of about 0.05 to 0.1 per degree. Zhu and MacDougall (1998) also reported data on coccolith oozes that were 1.88 to 2.64‰ lighter than seawater. De La Rocha and DePaolo (2000) reported data on one species of foraminifera that showed an average fractionation relative to seawater of -1.3‰ and a hint of a temperature dependence (Fig. 10). De La Rocha and DePaolo (2000) also reported data on cultured specimens of the coccolith *Emiliania huxleyi* and found the $\delta^{44}\text{Ca}$ values to be 1.3‰ lower than that of the seawater growth medium.

The most striking data yet published are those of Nagler et al. (2000), who provide evidence that cultured specimens of the foraminifer species *Globigerinoides sacculifer* exhibit a strongly temperature-dependent Ca isotope fractionation (Fig. 10). They proposed that this species could be used for ocean paleo-temperature determinations and demonstrated the application with analyses of separated *G. sacculifer* from a Late Pleistocene marine sediment core (Fig. 11a). Subsequent work by Gussone et al. (2003) on a different foraminifer species, *Orbulina universa* indicate that the temperature dependence of the Ca isotope fractionation in other foraminifera is much smaller than in *G. sacculifer* (Fig. 10). Data obtained by the author from bulk carbonate ooze from DSDP Site 590B (cf. Grant and Dickens 2002) show only small variations in $\delta^{44}\text{Ca}$ over the past 3 million years (Fig. 11b) and contrast with the *G. sacculifer* data. The Site 590B data may be recording small changes in the $\delta^{44}\text{Ca}$ of seawater or small shifts in local water temperature over this time period (see discussion below).

Gussone et al. (2003) were also able to demonstrate fractionation during inorganic precipitation of aragonite from a Ca-Mg-Cl solution and that the fractionation factor is temperature dependent (Fig. 10). The precipitation experiment involved diffusing CO_2 into a

Ca-Mg-Cl solution, which generates CaCO_3 precipitation as aragonite. Gussone et al. (2003) claim that the isotopic fractionation observed is a kinetic effect and imply that it is a result of differences in the diffusivity of isotopic species in solution. Although not explained in the paper, they infer that precipitation of aragonite is limited by the rate that dissolved Ca can diffuse to the surfaces of growing aragonite crystals. It is surprising that this process should have temperature dependence, because isotopic fractionation caused by aqueous diffusion should be a function only of the mass-dependent part of the diffusivity ratio as in Equation (3). Gussone et al. (2003) assume that they have measured a kinetic fractionation effect, but in fact they give no evidence that it is not an equilibrium fractionation. In any case, the results are important in that they demonstrate a behavior that mimics the fractionation in foraminifera with regard to temperature dependence, and a fractionation factor that is similar in size to that observed in both foraminifera and in vertebrate bone formation. For comparison, Skulan (1999) precipitated CaCO_3 from seawater at room temperature and estimated the fractionation factor to be smaller than that found by Gussone et al. (2003), only -0.2 to -0.4% .

Gussone et al. (2003) argue that the difference in fractionation behavior between foraminifera species may be explained by the way in which Ca ions are transported across cell membranes or through aqueous media by diffusion. The relatively small fractionation observed in *O. universa* and in inorganic aragonite precipitation suggests that the diffusing Ca species is an aquocomplex with a mass of about 600. This would require that the Ca^{2+} ions be associated with about 30 water molecules, or that they are in complexes involving both water molecules and anions. Gussone et al. (2003) suggest the reason that the temperature dependence of the fractionation in *G. sacculifer* is so large is that this organism dehydrates the Ca^{2+} ions before calcification so that the diffusing species is the Ca^{2+} ion. These conclusions are interesting but difficult to understand insofar as the absolute value of the kinetic fractionation factor for Ca isotopes should theoretically be dependent on the mass of the diffusing species, but the fractionation factor should theoretically have no temperature dependence. Hence the difference in the temperature dependence of the fractionation factor for different foraminifera species is not likely to be due to differences in the mass of the diffusing complex.

Calcium in the weathering cycle

The global calcium cycle is intimately linked to the carbon and nitrogen cycles. The weathering of Ca from silicates and its eventual sequestration in marine carbonates plays a major role in the control of atmospheric CO_2 concentrations (Berner et al. 1983; Raymo et al. 1988; Sundquist 1993). Calcium concentrations in the ocean have varied over geologic time. Kempe and Degens (1985) theorize that Ca^{2+} concentrations in the ocean were near zero from 4–1 Ga, whereas the modern day value is 10mM (Holland 1978; Broecker and Peng 1982). Models suggest secular variations in the marine Ca^{2+} concentration of seawater ranging from 10 to more than 40 mM during the Phanerozoic (Hardie 1996; Stanley and Hardie 1998), and these expectations are confirmed to some degree by studies of fluid inclusions in evaporite minerals (Horita et al. 2002; **Fig. 12**). Deposition rates of carbonate also vary widely. Massive carbonate deposition occurred during the late Cretaceous, for instance, following an extended period of deposition of carbonate-poor sediments (Kennett 1982).

To relate the isotopic composition of marine calcium to variations in the calcium cycle requires characterization of the $\delta^{44}\text{Ca}$ values of the sources and sinks of Ca to the oceans, and estimates of the Ca fluxes. Neither is well documented presently. Estimates of the calcium fluxes from Milliman (1993) are shown in **Table 3**. There are six analyses of $\delta^{44}\text{Ca}$ from mid-ocean ridge hydrothermal vents, and these average $+0.2 \pm 0.2$ (Zhu and MacDougall 1998; Schmitt et al. 2003b). There are five analyses of groundwater reported by Schmitt et al. (2003b), and those average $\delta^{44}\text{Ca} = -0.4 \pm 0.2$. There are no data for pore fluids from deep-sea sediments, but the $\delta^{44}\text{Ca}$ values of the diagenetic flux from sediments is expected to resemble the average value of carbonate ooze, which as described below is probably about -0.5 ± 0.2 .

The $\delta^{44}\text{Ca}$ values of riverine dissolved calcium show significant variability and correlate with $^{87}\text{Sr}/^{86}\text{Sr}$ (Fig. 13). The Eel River in Northern California has a high $\delta^{44}\text{Ca}$ value. The Ganges tributaries, which drain the Himalaya, have low $\delta^{44}\text{Ca}$ values. Insofar as the Himalayan Rivers also have extremely high $^{87}\text{Sr}/^{86}\text{Sr}$ ratios, the low $\delta^{44}\text{Ca}$ values may be partly attributable to the presence of excess radiogenic ^{40}Ca . Judging from the Sr isotopic data and the low published values of ϵ_{Nd} for the Himalayan granites (Deniel et al. 1987), the radiogenic ^{40}Ca excess could account for a shift of -0.2 to -0.4 in the $\delta^{44}\text{Ca}$ value (see Fig. 4). Zhu and MacDougall (1998) state that their $\delta^{44}\text{Ca}$ measurements account for variations in ^{40}Ca but they do not provide the data to demonstrate this. The Ganges tributaries represent an instance where separate analysis of radiogenic ^{40}Ca enrichments would be useful. Overall, the average $\delta^{44}\text{Ca}$ value of the riverine flux is not accurately determined. The value given in Table 3 is the approximate average value measured for large rivers.

At steady state the Ca isotopic composition of the inputs of calcium to the oceans should be identical to the outputs. Calcium is removed from the oceans by carbonate sedimentation. Measurements of bulk carbonate sediments are summarized in histogram format in Figure 14. Virtually all of the samples measured at the University of California, Berkeley (Skulan et al. 1997; De La Rocha and DePaolo 2000; and unpublished data from DSDP Site 590B), fall in the range $\delta^{44}\text{Ca} = +0.2$ to -0.9 . The mean and standard deviation are -0.5 ± 0.2 . Comparison to the river data (Fig. 12) shows that the deep sea carbonate mean value is slightly lower than river calcium, and slightly lower than the average value estimated for the total Ca input to the oceans (Table 3). The bulk carbonate ooze $\delta^{44}\text{Ca}$ data from Zhu and MacDougall (1998), however, are distinct from the Berkeley data, and the values are considerably lower than appears likely for the average input calcium.

The deduced average input $\delta^{44}\text{Ca}$ is not identical to the average volcanic rock value, but is lower by about 0.4% (Fig. 14). This suggests that weathering may discriminate between calcium isotopes. This inference is supported by the few available data on soils (Fig. 14; Skulan and DePaolo 1999; Skulan 1999; Schmitt et al. 2003b). The soils generally have $\delta^{44}\text{Ca}$ values that are higher than the volcanic rocks. Data to allow direct comparison of soils to parent rock material are not available.

For a simple model of Ca cycling, where the Ca sources for the ocean are weathering of continental rocks, pore fluids in the marine environment, and ocean floor basalt (Gieskes and Lawrence 1981; Berner et al. 1983; Elderfield et al. 1999), and the primary sink is the biological fixation of Ca into sediments, the rate of change of $\delta^{44}\text{Ca}$ ($= \delta_{\text{SW}}$) of the oceans is given by:

$$N_{\text{Ca}} \frac{d\delta_{\text{SW}}}{dt} = F_{\text{C}}(\delta_{\text{C}} - \delta_{\text{SW}}) + F_{\text{H}}(\delta_{\text{H}} - \delta_{\text{SW}}) - F_{\text{Sed}}\Delta_{\text{Sed}} \quad (5)$$

where N_{Ca} is the number of moles of Ca in the oceans, F_{C} is the continental (riverine and groundwater) weathering flux modified by the contributions of the marine diagenetic flux, F_{H} is the hydrothermal flux from mid-ocean ridges and off-ridge oceanic basalt weathering, F_{Sed} is the rate of biological removal of Ca into sediments, and Δ_{Sed} is the average fractionation factor for $\delta^{44}\text{Ca}$ associated with biological removal of Ca from the oceans. The steady state $\delta^{44}\text{Ca}$ of the ocean is given by:

$$\delta_{\text{SW}}(s.s.) = \frac{F_{\text{C}}\delta_{\text{C}} + F_{\text{H}}\delta_{\text{H}} - F_{\text{Sed}}\Delta_{\text{Sed}}}{F_{\text{C}} + F_{\text{H}}} \quad (6)$$

If the Ca concentration of the ocean is unchanging, then $F_{\text{Sed}} \approx F_{\text{C}} + F_{\text{H}}$, and the solution is:

$$\delta_{\text{SW}} = \delta_{\text{W}} - \Delta_{\text{Sed}} \quad (7)$$

where δ_{W} is the average value for all rock weathering fluxes including the hydrothermal flux.

The overall Ca isotope cycle is diagrammed in **Figure 15**. The average igneous rock has $\delta^{44}\text{Ca} \approx 0$ and the average carbonate rock has $\delta^{44}\text{Ca} \approx -0.5$. The calcium released from weathering of carbonate and silicate rocks probably has $\delta^{44}\text{Ca} \approx -0.4$ to -0.5 and the hydrothermal flux modifies this only slightly. The fractionation associated with calcium removal from the oceans is estimated to be $\Delta_{\text{Sed}} = -1.4 \pm 0.1$. Hence the expected steady state value for the $\delta^{44}\text{Ca}$ of the oceans is $+0.9$ to $+1.0$. Using these numbers, therefore, it appears that the current system is close to steady state, since the seawater value is in fact very close to $+1.0$ (De La Rocha and DePaolo 2000; Schmitt et al. 2003b). Zhu and MacDougall (1998), however, suggest that the value for Δ_{Sed} should be -2.2 ± 0.3 . If this number were used, then it would have to be concluded that the system is far from steady state. The Zhu and MacDougall (1998) carbonate ooze data are the only data available that suggest that Δ_{Sed} should be much different from -1.4 ± 0.1 . The fractionation studies (Fig. 10), as well as the studies of deep sea ooze and chalk by Skulan and DePaolo (1997), De La Rocha and DePaolo (2000), and the unpublished data shown in Figure 11b, all suggest that Δ_{Sed} is in the range -1.3 to -1.5 .

Ca isotopic variations in the paleo-oceans

As noted above, it is likely that the calcium input fluxes to the oceans and the outputs fluxes are not always equal. According to Equation (5), this means that the seawater $\delta^{44}\text{Ca}$ ratio can vary with time. The rapidity with which the seawater $\delta^{44}\text{Ca}$ can change is dictated by the residence time of calcium in seawater. At present, the residence time is estimated to be about 1 million years (e.g., Holland 1978). In the past, the residence time could have been larger or smaller, perhaps by as much as a factor of 5 or even 10, depending on the Ca concentration in seawater (Fig. 12) and the riverine, diagenetic and hydrothermal fluxes of calcium to the oceans.

The best method for reconstructing the seawater $\delta^{44}\text{Ca}$ in the geologic past has not been demonstrated. The work done so far has been mainly on bulk carbonate ooze and chalk, mainly of Cenozoic age, and the general features of the data have been corroborated by studies of marine phosphate (Schmitt et al. 2003a). The assumption is that the fractionation factor applicable to the formation of the carbonate sediments from seawater does not vary with time. De La Rocha and DePaolo (2000) reported the data shown in **Figure 16a** for Cenozoic carbonates. The data indicate that carbonate $\delta^{44}\text{Ca}$ values are not constant with time, and if one accepts that these sediment samples are globally representative, then this would suggest that the seawater values have also changed with time. The average spacing of the De La Rocha and DePaolo (2000) data is about 3 m.y. between 0 and 45 Ma. This spacing is longer than the nominal residence time and hence the data may be aliased. Much more closely spaced data are shown for the past 3 million years in Figure 11b, all from a single carbonate ooze section cored at DSDP Site 590B in the Tasman Sea (DePaolo, unpublished data). The Site 590B data show that on timescales less than 1 million years, there are only very small changes in the $\delta^{44}\text{Ca}$ of the bulk ooze, as expected if they are reflecting seawater variations.

The interpretation of the data from bulk oozes and chinks, even if it is accepted that they are providing a global signal, is different depending on whether the timescales of interest are greater than or smaller than the residence time of Ca. Equation (5) can be written also in the following form:

$$\frac{N_{\text{Ca}}}{F_{\text{W}}} \frac{d\delta_{\text{SW}}}{dt} = (\delta_{\text{W}} - \delta_{\text{SW}}) - \frac{F_{\text{Sed}}}{F_{\text{W}}} \Delta_{\text{Sed}} \quad (8)$$

where all of the inputs to the ocean have been lumped into a single weathering term. The amount of dissolved calcium in the oceans is described by:

$$\frac{dN_{Ca}}{dt} = F_W - F_{Sed} \quad (9)$$

In the case that $F_W = F_{Sed}$, and δ_W and Δ_{Sed} are constant, then Equation (7) will be satisfied, and δ_{SW} will be unchanging with time. At steady state it will also be the case that:

$$\delta_{Sed} = \delta_{SW} + \Delta_{Sed} = \delta_W \quad (10)$$

Hence, over the long term, the $\delta^{44}Ca$ of the sedimentation flux is not dependent on the fractionation factor, only on the $\delta^{44}Ca$ of the weathering flux. And overall, in the long term the $\delta^{44}Ca$ of the oceans and of sedimentary Ca is not expected to change unless the $\delta^{44}Ca$ of the weathering flux changes. The equations allow mainly for excursions from the weathering flux value due to shifts in Δ_{Sed} or F_W/F_{Sed} ; excursions that last for periods of time up to a few times the residence time (generally a few million years).

One way to temporarily change δ_{SW} is to change Δ_{Sed} , which is possible if there is sufficient change in ocean temperature (Fig. 10). Based on the lower slope curves from Figure 10, a temperature change of 5°C might generate a change of $\delta^{44}Ca$ of about 0.1‰. Local or even global changes in ocean temperature can happen quickly (hundreds to thousands of years), which is much faster than the ocean can change $\delta^{44}Ca$. Hence temperature fluctuations may produce small $\delta^{44}Ca$ fluctuations in the sediment on timescales short in comparison to the residence time of calcium. However, on long timescales, the oceans will change $\delta^{44}Ca$ to adjust to any change in Δ_{Sed} , whether it is due to temperature or some other effect such as a change in the mode of calcium removal from deep sea to shelf carbonates.

Changes in δ_W can generate changes in δ_{SW} that persist for time periods longer than the residence time. The restricted range in $\delta^{44}Ca$ in rocks suggests that δ_W changes are likely to be small (Schmitt et al. 2003a; De La Rocha and DePaolo 2000), but the relatively large range in the river $\delta^{44}Ca$ values (Fig. 13) suggests that it is indeed possible and perhaps likely that relatively long-term but small changes in δ_W occur.

Considering that there is geologic evidence that the Ca concentration of the oceans change with time, it is necessary that F_W/F_{Sed} changes with time. As noted by De La Rocha and DePaolo (2000), if the steady state equation for the sedimentary values is written as:

$$\delta_{Sed}(t) = \delta_W(t) - \Delta_{Sed} \left[\frac{F_{Sed}}{F_W}(t) - 1 \right] \quad (11)$$

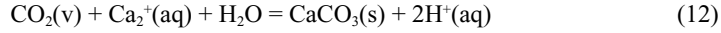
then it can be estimated that variations of δ_{Sed} of $\pm 0.4\text{‰}$, as suggested by the data, can be generated by variations of F_W/F_{Sed} from about 0.7 to 1.2 (Fig. 16b). If F_W/F_{Sed} is 1.2 and the residence time of Ca in the oceans is 1 m.y., then the ocean Ca concentration will double in a period of about 4 residence times. The timescale for doubling could be lengthened or shortened depending on whether the absolute values of the fluxes change at the same time that the ratio changes. The long timescales of the variations shown by De La Rocha and DePaolo (2000) data could only be explained by changes in either or both of F_W/F_{Sed} and δ_W .

Paleoclimatology

The small changes in $\delta^{44}Ca$ may turn out to be useful for characterizing past climates and climate changes. This can be illustrated by “straw man” analyses of the data in Figures 11b and 16. The only potentially significant signal in the Pleistocene 590B record is the slight drop in $\delta^{44}Ca$ between 0.8 and 0.4 Ma. Because of the short timescale, it is possible that this

represents cooling beginning at about 0.7 or 0.8 Ma. The longer-term variations shown in Figure 16a cannot be due to temperature changes. De La Rocha and DePaolo (2000) favored an interpretation in terms of changing F_w/F_{sed} . An important implication of such changes is the change of seawater Ca concentration.

The CO_2 concentration in the earth's atmosphere is ultimately governed by the calcium carbonate equilibrium in the ocean (e.g., Berner et al. 1983). If the oceans are in equilibrium with calcite, which is usually the case, then to a reasonable approximation, the pCO_2 of the atmosphere is defined by the equilibrium:



And therefore, pCO_2 is related to ocean pH and Ca^{2+} concentration by:

$$pCO_2 = \frac{[H^+]^2}{\ln K_{eq}(T)[Ca^{2+}]} \quad (13)$$

where K_{eq} is the equilibrium constant for equation (12). It has recently been proposed that boron isotopes allow reconstruction of past ocean pH values (Pearson and Palmer 2000). If Ca isotopes can help estimate changes in the ocean Ca concentration, then one can generate a fully constrained paleo- pCO_2 curve based on Equation (13).

The ratio of the fluxes of Ca into and out of the ocean can be reconstructed from the seawater $\delta^{44}Ca$ record using the relation (from Eqn. 8):

$$\frac{F_{sed}}{F_w} = \frac{1}{\Delta_{sed}} \left[\frac{N_{Ca}}{F_w} \frac{d\delta_{sw}}{dt} + (\delta_w - \delta_{sw}) \right] \quad (14)$$

Starting with present conditions, where $N_{Ca}/F_w \approx 1$ million years, and assuming that both Δ_{sed} and δ_w are constant, the past variations of F_{sed}/F_w are deduced as shown in Figure 16b. This curve does not uniquely determine the magnitude of past changes in $[Ca^{2+}]$, which can be seen from:

$$\frac{dN_{Ca}}{dt} = F_w \left(1 - \frac{F_{sed}}{F_w} \right) \quad (15)$$

With sufficiently closely spaced data such as those from Site 590B, it may be possible to estimate past variations in $[Ca^{2+}]$ by integrating Equation (15), and to combine that information with estimates of paleo-pH from B isotopes to calculate the expected changes in pCO_2 in the past. De La Rocha and DePaolo (2000) gave somewhat more general conclusions based on their data. For example, the high $\delta^{44}Ca$ in the Late Eocene corresponds to a period of relatively high global temperature as suggested by the low foraminiferal $\delta^{18}O$ values (Fig. 16c). The high $\delta^{44}Ca$ corresponds to excess sedimentation or a decreased weathering flux, which suggests decreasing $[Ca^{2+}]$ and hence increasing pCO_2 . The Oligocene is a period of lower global temperatures, and the relatively low $\delta^{44}Ca$ indicates increasing $[Ca^{2+}]$ and hence decreasing pCO_2 .

A bolder approach is to integrate the curve in Figure 16b to estimate past ocean $[Ca^{2+}]$ variations and combine these with estimates of paleo-pH from boron isotope data. This exercise does not yield tight constraints on past atmospheric CO_2 levels because the $[Ca^{2+}]$ estimates are too sensitive to the assumptions (and there are too few data), but helps to illustrate how the parameters of the Ca cycle are related to other observations. **Figure 17a** shows the variations of seawater $[Ca^{2+}]$ over the past 60 million years based on the data of Figure 16a and for three different assumed values of the $\delta^{44}Ca$ value of the weathering flux.

Varying the assumed values of Δ_{sed} and the Ca residence time (see Eqn. 14) has much less effect on the results. The $[\text{Ca}^{2+}]$ estimates become highly uncertain with increasing age. However, it is interesting to note that the estimates of paleo-seawater $[\text{Ca}^{2+}]$ given by Horita et al. (2002; see Fig. 12) are most compatible with a relatively low value of δ_w . This observation can be taken as support for the idea that the weathering flux has $\delta^{44}\text{Ca}$ that is significantly different from average igneous rocks, and hence that light Ca is preferentially released from rocks by weathering processes. When the $[\text{Ca}^{2+}]$ values are combined with the paleo-pH values of Pearson and Palmer (2000) (Fig. 17b), the result is the paleo- pCO_2 curves shown in Figure 17c. The curve for $\delta_w = -0.5$ is similar to the curve produced by Pearson and Palmer (2000), who assumed that $[\text{Ca}^{2+}]$ is proportional to seawater alkalinity. This curve also shows similarities to what might be expected from $\delta^{18}\text{O}$ and other evidence (e.g., Fig. 16c). The early Cenozoic is a time of high but variable pCO_2 . By early Miocene time (ca. 22 Ma) CO_2 levels are comparable to the present (pre-industrial) values. The calculated pCO_2 for the period from the middle Miocene through the Pliocene comes out lower than the modern value, which does not correspond well with the $\delta^{18}\text{O}$ evidence for continued cooling between 15 Ma and the present (Fig. 16c). It may be noteworthy that higher assumed values for δ_w correspond to very high levels of atmospheric CO_2 in the early Cenozoic, whereas δ_w values in the range -0.5 to -0.6 correspond to the $1\times$ to $10\times$ higher CO_2 levels that are typically estimated with other approaches (e.g., Ekart et al. 1999).

CONCLUSIONS AND IMPLICATIONS

The research summarized here demonstrates that there are significant and systematic variations in the Ca isotopic composition of geological and biological materials. Most if not all of the natural isotopic fractionation has been interpreted in terms of kinetically controlled processes, but there has not yet been any measurement of the equilibrium isotopic partitioning. Laboratory studies demonstrate that some inorganic processes—diffusive transport in silicate liquids and precipitation of aragonite from aqueous solution—can fractionate Ca isotopes. In nature the effects of inorganic fractionation of Ca isotopes have not been demonstrated. Organic processes, however, clearly do fractionate Ca isotopes and hence the Ca isotope system may have its greatest geochemical value as a tracer of organic processes in the geologic record. There also appears to be a role for Ca isotopes in studies of the metabolism of higher organisms and for intracellular ion transport. The research to date suggests that Ca isotopes are fractionated within organisms mainly in the process of formation of mineral matter in bone or shell material.

Calcium also has isotopic variations stemming from the radioactive decay of ^{40}K to ^{40}Ca . These variations can be used for geochronology and may also be useful for studies of rock weathering, soil formation, magma genesis, diagenesis, and metamorphism.

The observed range of natural variations of $\delta^{44}\text{Ca}$ is about 4 to 5‰ in terrestrial materials and up to 50‰ in high temperature condensate minerals in carbonaceous chondrites. The typical reproducibility of measurements is about $\pm 0.15\text{‰}$. Broader application of Ca isotope measurements in geochemistry may be possible, particularly if the reproducibility can be improved to $\pm 0.05\text{‰}$ to 0.03‰ . There is hope that this can be achieved either with inductively coupled plasma source mass spectrometry (Halicz et al. 1999) or with a new generation of multi-collector thermal ionization mass spectrometers (Heuser et al. 2002).

Studies of the global calcium cycle with isotopes have promise but require further characterization of the components of the cycle—rocks, soils, rivers, sediments, organic material—to be fully realized. Study of the calcium cycle is complementary to studies of the carbon cycle, and may contribute to understanding past Earth climates and oceans. The fractionation factors for Ca isotopes, their causes, magnitude, temperature dependence

and ubiquity in metabolic processes, are still poorly understood. Further studies may yield information on metabolism, Ca complexing in aqueous solutions, and polymerization in silicate melts. Studies of vertebrates suggest that significant Ca isotopic variations may be generated in soft tissue during bone mass loss, and whenever the dietary Ca supply is small in comparison to Ca demand.

ACKNOWLEDGMENTS

The manuscript was significantly improved as a result of reviews by Brian Marshall and Tom Bullen. The author's recent work on Ca isotopes has been supported largely by the Director, Office of Energy Research, Basic Energy Sciences, Chemical Sciences, Geosciences and Biosciences Division of the U.S. Department of Energy under Contract No. De-AC03-76SF00098 to the E.O. Lawrence Berkeley National Laboratory, and by the National Science Foundation, most recently by grant number EAR-9909639.

REFERENCES

- Ahrens LH (1951) The feasibility of a calcium method for the determination of geological age. *Geochim Cosmochim Acta* 1:312-316
- Baadsgaard H (1987) Rb–Sr and K–Ca isotope systematics in minerals from Potassium horizons in the Prairie Evaporite Formation, Saskatchewan, Canada. *Chem Geol Isotope Geosci Sec* 66:1-15
- Beckinsale RD, Gale NM (1969) A reappraisal of the decay constants and branching ratio of ^{40}K . *Earth Planet Sci Lett* 6:289-294
- Barker F, Hedge C, Millard H, O'Neil J (1976) Pikes Peak Batholith: Geochemistry of some minor elements and isotopes, and implications for magma genesis. *In: Studies in Colorado Field Geology*. Vol 8. Weimer RJ (ed) Colorado School of Mines Professional Contributions, Colorado, p 44-56
- Berner RA, Lasaga AC, Garrels RM (1983) The carbonate-silicate geochemical cycle and its effect on atmospheric carbon dioxide over the past 100 million years. *Amer J Sci* 283:641-683
- Blum JD, Erel Y (1997) Rb-Sr isotope systematics of a granitic soil chronosequence: The importance of biotite weathering. *Geochim Cosmochim Acta* 61:3193-3204
- Broecker W, Peng TH (1982) *Tracers in the Sea*. Eldigio Press, Palisades NY
- Cameron AGW (1979) From nucleosynthesis to the birth of the Earth; origin of the planets and of the Earth. *In: The rediscovery of the Earth*. Motz L (ed) Van Nostrand Reinhold New York, p 51-58
- Chen CH, Nakada S, Shieh YN, DePaolo DJ (1999) The Sr, Nd and O isotopic studies of the 1991-1995 eruption at Unzen. *Japan J Volc Geothermal Res* 89:243-253 (1999)
- Clayton RN, Hinton RW, Davis AM (1988) Isotopic variations in the rock-forming elements in meteorites. *Phil Trans R Soc Lond A325*:483-501
- Clementz MT, Holden P, Koch PL (2003) Are calcium isotopes a reliable monitor of trophic level in marine settings? *Int J Osteoarchaeology* 13(1-2):29-36
- Coleman ML (1971) Potassium–calcium dates from pegmatitic micas. *Earth Planet Sci Lett* 12:399-405
- Condie KC (1993) Chemical composition and evolution of the upper continental crust: contrasting results from surface samples and shales. *Chem Geol* 104:1-37
- Davis AM, Hashimoto A, Clayton RN, Mayeda TK (1990) Isotope mass fractionation during evaporation of Mg_2SiO_4 . *Nature* 347:655-658
- Davis AM, MacPherson GJ (1996) Thermal processing in the solar nebula: Constraints from refractory inclusions. *In: Chondrules and the Protoplanetary Disk*. Hewins RH, Jones RH, Scott ERD (eds) Cambridge University Press, New York, p 71–76
- De La Rocha CL, DePaolo DJ (2000) Isotopic evidence for variations in the marine calcium cycle over the Cenozoic. *Science* 289(5482):1176-1178
- Deniel D, Vidal P, Fernandez A, LeFort P, Peucat JJ (1987) Isotopic study of the Manaslu granite (Himalaya, Nepal): inference on the age and source of Himalayan leucogranites. *Contrib Mineral Petrol* 96:78-92
- DePaolo DJ (1986) Detailed record of the Neogene Sr isotopic evolution of seawater from DSDP Site 590B. *Geology* 14:103-106
- Edmond JM (1992) Himalayan tectonics, weathering processes, and the strontium isotope record in marine limestones. *Science* 258:1594-1597
- Elderfield H, Wheat CG, Mottl MJ, Monnin C, Spiro B (1999) Fluid and geochemical transport through oceanic crust; a transect across the eastern flank of the Juan de Fuca Ridge. *Earth Planet Sci Lett* 172:151-165
- Eiler JM, Valley JW, Stolper EM (1996) Oxygen isotope ratios in olivine from the Hawaii Scientific Drilling Project. *J Geophys Res-Solid Earth*. 101(B5):11807-11813
- Eiler JM, Farley KA, Valley JW, Hauri E, Craig H, Hart SR, Stolper EM (1997) Oxygen isotope variations in ocean island basalt phenocrysts. *Geochim Cosmochim Acta* 61:2281-2293
- Ekar DD, Cerling TE, Montanez IP, Tabor NJ (1999) A 400 million year carbon isotope record of pedogenic carbonate: Implications for paleoatmospheric carbon dioxide. *Amer J Sci* 299:805-827
- Elderfield H, Schultz, A (1996) Mid-ocean ridge hydrothermal fluxes and the chemical composition of the ocean. *Ann Rev Earth Planet Sci* 24:191-224
- Fletcher IR, McNaughton NJ, Pidgeon RT, Rosman KJR (1997a) Sequential closure of K-Ca and Rb-Sr isotopic systems in Archaean micas. *Chem Geol* 138:289–301
- Fletcher IR, Maggi AL, Rosman KJR, McNaughton NJ (1997b) Isotopic abundance measurements of K and Ca using a wide-dispersion multi-collector mass spectrometer and low-fractionation ionisation techniques. *Int J Mass Spectrom Ion Proc* 163(1-2):1-17
- Getty SJ, DePaolo DJ (1995) Quaternary geochronology by the U-Th-Pb method. *Geochim Cosmochim Acta* 59:3267-3272

- Gieskes JM, Lawrence JR (1981) Alteration of volcanic matter in deep sea sediments: Evidence from the chemical composition of interstitial waters from deep sea drilling cores. *Geochim Cosmochim Acta* 45:1687-1703
- Grant KM, Dickens GR (2002) Coupled productivity and carbon isotope records in the southwest Pacific Ocean during the late Miocene-early Pliocene biogenic bloom. *Paleogeography, Paleoclimatology, Paleoceanography* 187:61-82
- Gussone N, Eisenhauer A, Heuser A, Dietzel M, Bock B, Bohm F, Spero H, Lea D, Buma J, Nagler, TF (2003) Model for kinetic effects on calcium isotope fractionation ($\delta^{44}\text{Ca}$) in inorganic aragonite and cultured planktonic foraminifera. *Geochim Cosmochim Acta* 67:1375-1382
- Halicz L, Galy A, Belshaw NS, O'Nions RK (1999) High precision measurement of calcium isotopes in carbonates and related materials by multiple collector inductively coupled plasma mass spectrometry (MC-ICP-MS). *J Anal Atom Spectr* 14:1835-1838
- Hardie LA (1996) Secular variation in seawater chemistry: An explanation for the coupled secular variation in the mineralogies of marine limestones and potash evaporites over the past 600 m.y. *Geology* 24:279-283
- Herzog LF (1956) Rb-Sr and K-Ca analyses and ages. *In: Nuclear processes in geologic settings*. Natl Research Council, Comm Nuclear Sci, Nuclear Sci Ser Rept 19:114-130
- Heuser A, Eisenhauer A, Gussone N, Bock B, Hansen BT, Nagler TF (2002) Measurement of calcium isotopes ($\delta^{44}\text{Ca}$) using a multicollector TIMS technique. *Int J Mass Spec* 220:387-399
- Hippler D, Schmitt A-D, Gussone N, Heuser A, Stille P, Eisenhauer A, Nagler T (2003) Calcium isotopic composition of various reference materials and seawater. *Geostandards Newsletter* 27:13-19
- Holland HD (1978) *The Chemistry of the Atmosphere and Oceans*. John Wiley and Sons, New York
- Holland HD (1984) *The Chemical Evolution of the Atmosphere and Oceans*. Princeton University Press, Princeton NJ
- Horita J, Zimmermann H, Holland HD (2002) Chemical evolution of seawater during the Phanerozoic: implications from the record of marine evaporates. *Geochim Cosmochim Acta* 66:3733-3756
- Inghram MG, Brown H, Patterson C, Hess DC (1950) The branching ratio of K-40 radioactive decay. *Phys Rev* 80:916-917
- Ireland TR, Fahey AJ, Zinner EK (1991) Hibonite-bearing microspherules; a new type of refractory inclusions with large isotopic anomalies. *Geochim Cosmochim Acta* 55:367-379
- Johnson CM, Beard BL (1999) Correction of instrumentally produced mass fractionation during isotopic analysis of Fe by thermal ionization mass spectrometry. *Int J Mass Spect* 193:87-99
- Jungeck MHA, Shimamura T, Lugmair GW (1984) Calcium isotope variations in Allende. *Geochim Cosmochim Acta* 48:2651-2658
- Kempe S, Degens ET (1985) An early soda ocean? *Chemical Geology* 53:95-108
- Kennett J (1982) *Marine Geology*. Prentice-Hall, Englewood Cliffs NJ
- Lee T, Papanastassiou DA, Wasserburg GJ (1977) Mg and Ca isotopic study of individual microscopic crystals from the Allende meteorite by the direct loading technique. *Geochim Cosmochim Acta* 41:1473-1485
- Lee T, Russell WA, Wasserburg GJ (1979) Calcium isotopic anomalies and the lack of aluminum-26 in an unusual Allende inclusion. *Appl J Lett* 228(L93-L98):661-662
- Marshall BD, DePaolo DJ (1982) Precise age determinations and petrogenetic studies using the K-Ca method. *Geochim Cosmochim Acta* 46:2537-2545
- Marshall BD (1984) *The potassium-calcium geochronometer*. PhD Dissertation, University of California, Los Angeles
- Marshall BD, Woodard HH, Krueger HW, DePaolo DJ (1986) K-Ca-Ar systematics of authigenic sanidine from Waukau, Wisconsin, and the diffusivity of argon. *Geology* 14:936-938
- Marshall BD, DePaolo DJ (1989) Calcium isotopes in igneous rocks and the origin of granite. *Geochim Cosmochim Acta* 53:917-922
- Milliman JD (1993) Production and accumulation of calcium carbonate in the ocean: budget of a non-steady state. *Global Geochem Cycles* 7:927-957
- McCauley S, DePaolo DJ (1997) The marine $^{87}\text{Sr}/^{86}\text{Sr}$ and ^{18}O records, Himalayan alkalinity fluxes and Cenozoic climate models. *In: Tectonic Uplift and Climate Change*. Ruddiman WF (ed) Plenum, New York, p 427-467
- Nagler TF, Villa IM (2000) In pursuit of the ^{40}K branching ratios: K-Ca and ^{39}Ar - ^{40}Ar dating of gem silicates. *Chem Geol* 169:5-16
- Nagler TF, Eisenhauer A, Muller A, Hemleben C, Kramers J (2000) The $\delta^{44}\text{Ca}$ -temperature calibration on fossil and cultured Globigerinoides sacculifer: New tool for reconstruction of past sea surface temperatures. *Geochem Geophys Geosys* 1(2000GC000091)
- Nelson DR, McCulloch MT (1989) Petrogenic applications of the ^{40}K - ^{40}Ca radiogenic decay scheme—a reconnaissance study. *Chem Geol (Isot Geosci Sect)* 79:275-293

- Niederer FR, Papanastassiou DA (1984) Ca isotopes in refractory inclusions. *Geochim Cosmochim Acta* 48:1279-1293
- Platzner I, Degani N (1990) Fractionation of stable calcium isotopes in tissues of date palm trees. *Biomed Environ Mass Spect* 19:822-824
- Pearson PN, Palmer MR (2000) Atmospheric carbon dioxide concentrations over the past 60 million years. *Nature* 406:695-699
- Polevaya NI, Titov NE, Belyaer VS, Sprintsson VD (1958) Application of the calcium method in the absolute age determination of sylvites. *Geochemistry* 8:897-906
- Raymo ME, Ruddiman WF (1992) Tectonic forcing of late Cenozoic climate. *Nature* 359:117-122.
- Renne PR, Swisher DD, Deino AL, Karner DB, Owens TL, DePaolo DJ (1998) Intercalibration of standards, absolute ages and uncertainties in $^{40}\text{Ar}/^{39}\text{Ar}$ dating. *Chem Geol* 145:117-152
- Richter FM, Rowley DB, DePaolo DJ (1992) Sr isotope evolution of sea water: the role of tectonics. *Earth Planet Sci Lett* 109:11-23
- Richter FM, Davis AM, Ebel DS, Hashimoto A (2002) Elemental and isotopic fractionation of Type B calcium-, aluminum-rich inclusions: Experiments, theoretical considerations, and constraints on their thermal evolution. *Geochim Cosmochim Acta* 66:521-540
- Richter FM, Davis AM, DePaolo DJ, Watson EB (2003) Isotope fractionation by chemical diffusion between molten basalt and rhyolite. *Geochim Cosmochim Acta* (*in press*) (2003)
- Rudnick RL, Fountain DM (1995) Nature and composition of the continental crust—a lower crustal perspective. *Rev Geophys* 33:267-309
- Russell SS, Huss GR, Fahey AJ, Greenwood RC, Hutchison R, Wasserburg GJ (1998) An isotopic and petrologic study of calcium-aluminum-rich inclusions from CO_3 meteorites. *Geochim Cosmochim Acta* 62:689-714
- Russell WA, Papanastassiou DA, Tombrello TA, Epstein S (1977) Ca isotope fractionation on the moon. *Proc. Lunar Sci. Conf.* 8th, 3791-3805.
- Russell WA, Papanastassiou DA (1978a) Calcium isotope fractionation in ion-exchange chromatography. *Anal Chem* 50:1151-1153
- Russell WA, Papanastassiou DA, Tombrello TA (1978b) Ca isotope fractionation on the Earth and other solar system materials. *Geochim Cosmochim Acta* 42:1075-1090
- Schärer U, Allègre CJ (1982) Uranium-lead system in fragments of a single zircon grain. *Nature* 295:585-587
- Schmitt AD, Bracke G, Stille P, Kiefel B (2001) The calcium isotope composition of modern seawater determined by thermal ionisation mass spectrometry. *Geostandard Newsletter* 25:267-275
- Schmitt A-D, Stille P, Venneman T (2003a) Variations of the $^{44}\text{Ca}/^{40}\text{Ca}$ ratio in seawater during the past 24 million years: evidence from $\delta^{44}\text{Ca}$ and $\delta^{18}\text{O}$ values of Miocene phosphates. *Geochim Cosmochim Acta* 67:2607-2614
- Schmitt AD, Chabaux F, Stille P (2003b) The calcium riverine and hydrothermal isotopic fluxes and the oceanic calcium mass balance. *Earth Planet Sci Lett* 6731:1-16
- Shaw DM, Cramer JJ, Higgins MD, Truscott MG (1986) Composition of the Canadian Precambrian Shield and the continental crust of the Earth. *In: The Nature of the Lower Continental Crust.* Dawson JB, Carswell DA, Hall J, Wedepohl KH (eds) Geological Society Special Publications 24:275-282
- Shih C-Y, Nyquist LE, Wiesmann H, (1994) K-Ca and Rb-Sr dating of two lunar granites: relative chronometer resetting. *Geochim Cosmochim Acta* 58:3101-3116
- Shu FH, Shang H, Lee T (1996) Toward an astrophysical theory of chondrites. *Science* 271:1545-1552
- Sims KWW, DePaolo DJ, Murrell MT, Baldrige WS, Goldstein S, Clague D, Jull M (1999) Porosity of the melting zone and variations in solid mantle upwelling rate beneath Hawaii: inferences from ^{238}U - ^{230}Th - ^{226}Ra and ^{235}U - ^{231}Pa . *Geochim Cosmochim Acta* 63:4119-4138
- Skulan JL (1999) Calcium isotopes and the evolution of terrestrial reproduction in vertebrates. PhD Dissertation, University of California, Berkeley
- Skulan J, DePaolo DJ, Owens TL (1997) Biological control of calcium isotopic abundances in the global calcium cycle. *Geochim Cosmochim Acta* 61:2505-2510
- Skulan J, DePaolo DJ (1999) Calcium isotope fractionation between soft and mineralized tissues as a monitor of calcium use in vertebrates. *Proc Nat Acad Sci* 96:13,709-13,713
- Smith DR, Noble J, Wobus RA, Unruh D, Douglass J, Beane R, Davis C, Goldman S, Kay G, Gustavson B, Saltoun B, Stewart J (1999) Petrology and geochemistry of late-stage intrusions of the A-type, mid-Proterozoic Pikes Peak batholith (Central Colorado, USA): implications for petrogenetic models. *Precambrian Res* 98:271-305
- Stanley SM, Hardie LA (1998) Secular oscillations in the carbonate mineralogy of reef-building and sediment-producing organisms driven by tectonically forced shifts in seawater chemistry. *Palaeogeography Palaeoclimatology Palaeoecology* 144:3-19

- Steiger RH, Jager E (1977) Subcommittee on geochronology: convention on the use of decay constants in geo- and cosmochemistry. *Earth Planet Sci Lett* 36:359-362
- Sundquist ET (1993) The global carbon dioxide budget. *Science* 259:934-941
- Taylor SR, McLennan SM (1995) The geochemical evolution of the continental crust. *Rev Geophys* 33:241-265
- Weber D, Zinner E, Bischoff A (1995) Trace element abundances and magnesium, calcium, and titanium isotopic compositions of grossite-containing inclusions from the carbonaceous chondrite Acfer 182. *Geochim Cosmochim Acta* 59:803-823
- Wedepohl KH (1995) The composition of the continental crust. *Geochim Cosmochim Acta* 59:1217-1239
- White AF, Blum AE, Schulz MS, Bullen TD, Harden JW, Peterson ML (1996) Chemical weathering rates of a soil chronosequence on granitic alluvium: I. Quantification of mineralogical and surface area changes and calculation of primary silicate reaction rates. *Geochim Cosmochim Acta* 60:2533-2550
- Wilkinson BH, Algeo TJ (1989) Sedimentary carbonate record of calcium-magnesium cycling. *Am J Sci* 289:1158-1194
- Zachos J, Pagani M, Sloan L, Thomas E, Billups K (2001) Trends, rhythms, and aberrations in global climate 65 Ma to present. *Science* 292:686-693
- Zhu P, Macdougall JD (1998) Calcium isotopes in the marine environment and the oceanic calcium cycle. *Geochim Cosmochim Acta* 62:1691-1698

Table 1. Natural abundances, measured isotope ratios, and enrichment factors used for Calcium isotopes.

Approximate isotopic abundances	
⁴⁰ Ca	96.98%
⁴² Ca	0.642%
⁴³ Ca	0.133%
⁴⁴ Ca	2.056%
⁴⁶ Ca	0.003%
⁴⁸ Ca	0.182%
Accepted “normal” isotopic ratios (Russell et al. 1978b; Niederer and Papanastassiou 1984)	
⁴⁰ Ca/ ⁴⁴ Ca = 47.153 ± 3 (can vary due to radiogenic ⁴⁰ Ca)	
⁴² Ca/ ⁴⁴ Ca = 0.31221 ± 2	
⁴³ Ca/ ⁴⁴ Ca = 0.06486 ± 1	
⁴⁶ Ca/ ⁴⁴ Ca = 0.001518 ± 2	
⁴⁸ Ca/ ⁴⁴ Ca = 0.088727 ± 9	
⁴⁴ Ca/ ⁴⁰ Ca = 0.0212076 ± 13	
⁴⁰ Ca/ ⁴² Ca = 151.016* ± 0.008 (Earth’s mantle value)	
*normalized to ⁴² Ca/ ⁴⁴ Ca = 0.31221	
For stable isotope fractionation studies (Skulan et al. 1997)	
$\delta^{44}\text{Ca} = 1000 \left(\frac{{}^{44}\text{Ca} / {}^{40}\text{Ca}_{\text{sample}}}{{}^{44}\text{Ca} / {}^{40}\text{Ca}_{\text{std}}} - 1 \right) = 1000 \left(\frac{{}^{44}\text{Ca} / {}^{40}\text{Ca}_{\text{sample}}}{0.0212076} - 1 \right)$	
For radiogenic ⁴⁰Ca enrichment studies (Marshall and DePaolo 1982)	
$\epsilon_{\text{Ca}} = 10000 \left(\frac{{}^{40}\text{Ca} / {}^{42}\text{Ca}_{\text{sample}}}{{}^{40}\text{Ca} / {}^{42}\text{Ca}_{\text{std}}} - 1 \right) = 10000 \left(\frac{{}^{40}\text{Ca} / {}^{42}\text{Ca}_{\text{sample}}}{151.016} - 1 \right)$	

Table 2. Calcium isotopic compositions of terrestrial volcanic rocks,
with other related isotopic parameters.

Sample Number	CaO (wt.%)	$\delta^{18}\text{O}$	$\delta^{44}\text{Ca}$	$\pm 2\text{s}$	ϵ_{Nd}	$^{87}\text{Sr}/^{86}\text{Sr}$	Sample Description (Ref.)
D54G	11.32	5.22	-0.33	0.07			Basalt, Marianas dredge (1)
KOO-10	8.13	5.71	-0.17	0.22			Tholeiitic Basalt, Koolau (1)
KOO-21	8.39	5.99	-0.10	0.19		0.70426	Tholeiitic Basalt, Koolau (1)
KOO-55	8.64	5.75	-0.09	0.14		0.70416	Tholeiitic Basalt, Koolau (1)
GUG-6	10.82	5.03	0.21	0.22	7.9		Basalt, Marianas (1)
ALV-1833	11.68	5.10	-0.17	0.23	8.3	0.70293	Basalt, Marianas (1)
HK-02	10.18		-0.16	0.26	7.7	0.70325	Alkali basalt, Haleakala (2)
HU-24	9.42		-0.32	0.23	5.7	0.70357	Alkali basalt, Hualalai (2)
HK-11	9.67		-0.37	0.27	8.2	0.70310	Alkali basalt, Haleakala (2)
HU-05	10.09		0.14	0.16	5.2	0.70360	Alkali basalt, Hualalai (2)
HSDP 452	10.46	4.80	-0.16	0.12	6.9	0.70358	Tholeiitic basalt Mauna Kea (1)
HSDP 160	10.45	4.87	0.34	0.25	7.3	0.70350	Alkali basalt, Mauna Kea (1)
92-12-29	4.89		-0.15	0.22	1.6	0.70446	Unzen Dacite (1992 eruption) (3)
94-02-05	4.91		0.02	0.24	1.4	0.70446	Unzen Dacite (1994 eruption) (3)
76DSH-8	5.35		0.12	0.21		0.70309	Shasta Dacite (Black Butte) (4)
76DSH-8	5.35		-0.11	0.21		0.70309	Shasta Dacite, Hornblende (4)
76DSH-8	5.35		-0.27	0.06		0.70309	Shasta Dacite, Plagioclase (4)
92DLV-113	0.53		-0.09	0.20	-0.3	0.70611	Inyo rhyolite
IO-14	11.82		-0.16	0.19			Basalt , Indian Ocean MORB
IO-38	11.30		-0.23	0.10			Basalt , Indian Ocean MORB
SUNY MORB	10.38		-0.22	0.03			MORB (5)
SUNY MORB	10.38		-0.27	0.12			MORB (5)
Lake Co. Obsidian	0.53		-0.23	0.05			Rhyolite (5)

References: (1) Eiler et al. (1996, 1997); (2) Sims et al. (1999); (3) Chen et al. (1999); (4) Getty and DePaolo (1995); (5) Richter et al. (2003)

Table 3. Modern marine Ca²⁺ budget*

Inputs	Flux (Tmol y⁻¹)	δ⁴⁴Ca (‰)
Riverine	12-15	-0.2 ± 0.2
Diagenetic	3-5	-0.5 ± 0.2
Groundwater	5-16	-0.4 ± 0.2
Hydrothermal	2-3	+0.2 ± 0.2
Aeolian	<0.05	-0.1 ?
Total	23 to 40	-0.3 ± 0.2
Outputs		
Biogenic Carbonate	32	-0.4 ± 0.2**

*Fluxes are based on Milliman (1993). Estimates of δ⁴⁴Ca were compiled from Skulan et al. (1997), Zhu and MacDougall (1998), De La Rocha and DePaolo (2000), Schmitt et al. (2003b), and DePaolo (unpublished data).

**Based on Pleistocene and younger deep sea ooze data of De La Rocha and DePaolo (2000) and DePaolo (unpublished; see Fig. 11b). Zhu and MacDougall (1998) estimate this value as about -1.2 ± 0.3.

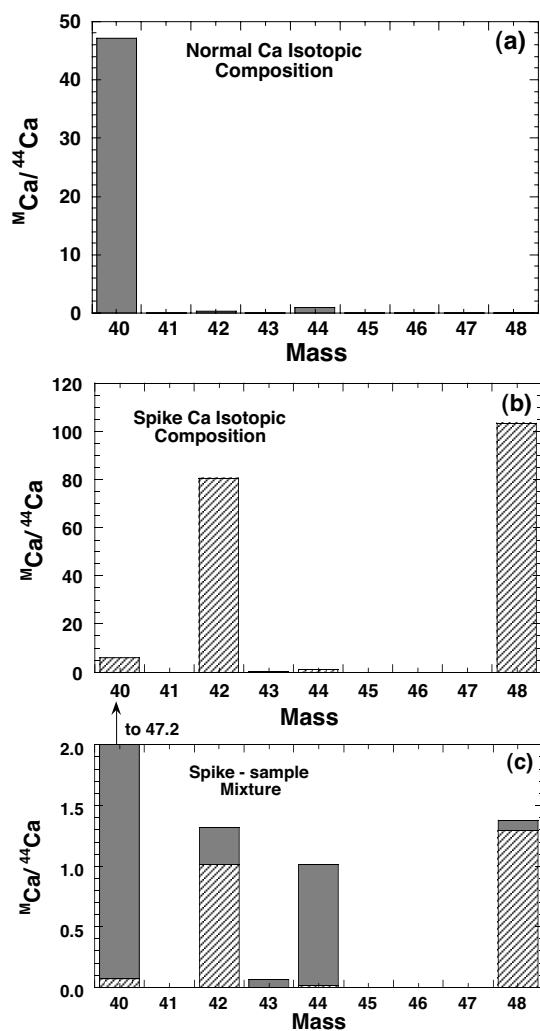


Figure 1. Schematic representation of the calcium mass spectrum in (a) natural materials, (b) a ^{42}Ca - ^{48}Ca tracer solution used for separating natural mass dependent isotopic fractionation from mass discrimination caused by thermal ionization, and (c) a typical mixture of natural calcium and tracer calcium used for analysis. The tracer solution has roughly equal amounts of ^{42}Ca and ^{48}Ca . In (c) the relative isotopic abundances are shown with an expanded scale. Note that in the mixed sample, masses 42 and 48 are predominantly from the tracer solution, and masses 40 and 44 are almost entirely from natural calcium. This situation enables the instrumental fractionation to be gauged from the $^{42}Ca/^{48}Ca$ ratio, and the natural fractionation to be gauged from the sample $^{44}Ca/^{40}Ca$ ratio.

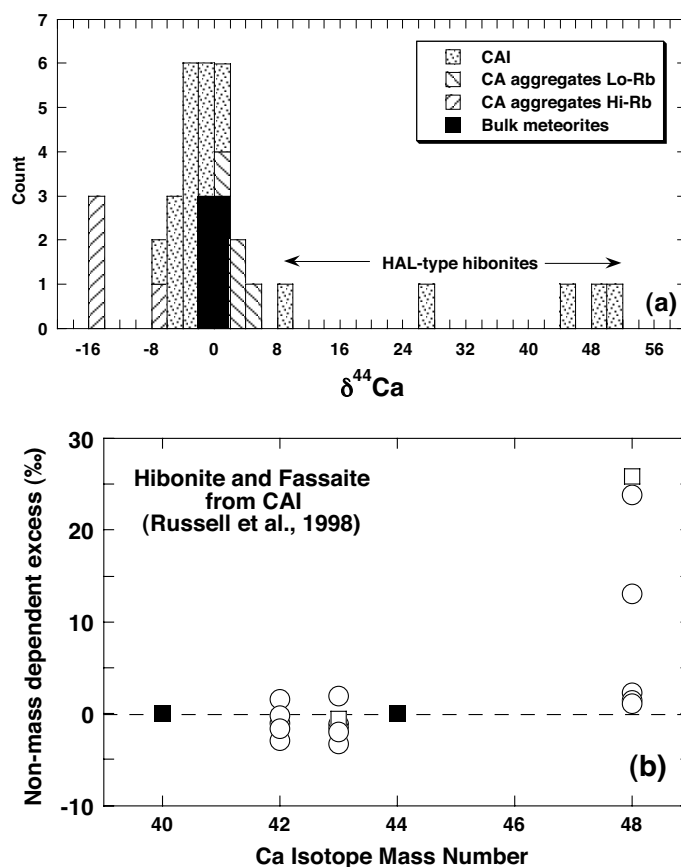


Figure 2. (a) Histogram of $\delta^{44}\text{Ca}$ values measured for samples from calcium-aluminum rich inclusions (CAI), calcium-aluminum rich aggregates from the Allende meteorite by Niederer and Papanastassiou (1984) and Lee et al. (1977, 1979), and bulk meteorites by these authors as well as Russell et al. (1978). Bulk meteorites cluster within about $\pm 1\%$ of $\delta^{44}\text{Ca} = 0$, which is also the value that characterizes terrestrial igneous rocks (see Figs. 5 and 14). The large effects in Ca-Al rich samples have been interpreted as resulting from evaporation of silicate liquid in the early Solar Nebula at high temperature under non-equilibrium conditions, and recondensation of vapor enriched in light Ca isotopes. The large positive $\delta^{44}\text{Ca}$ values are from hibonite from CAI's and are most likely indicative of residual material that has been affected by partial evaporation. The Ca-Al aggregates have both high and low $\delta^{44}\text{Ca}$, which tends to correlate with the amount of the volatile element Rb. (b) Examples of ^{48}Ca excess due to nucleosynthetic processes. These data were obtained by ion microprobe measurements of the minerals hibonite (circles) and fassaite (squares) from calcium-aluminum rich inclusions in type CO3 meteorites (Russell et al., 1998). The values shown represent isotopic ratios that have been corrected for mass dependent fractionation using the $^{44}\text{Ca}/^{40}\text{Ca}$ ratio (hence both ^{40}Ca and ^{44}Ca plot at zero); the other plotted values are residuals that cannot be explained by mass dependent fractionation. Typical uncertainty for these measurements is $\pm 4\%$.

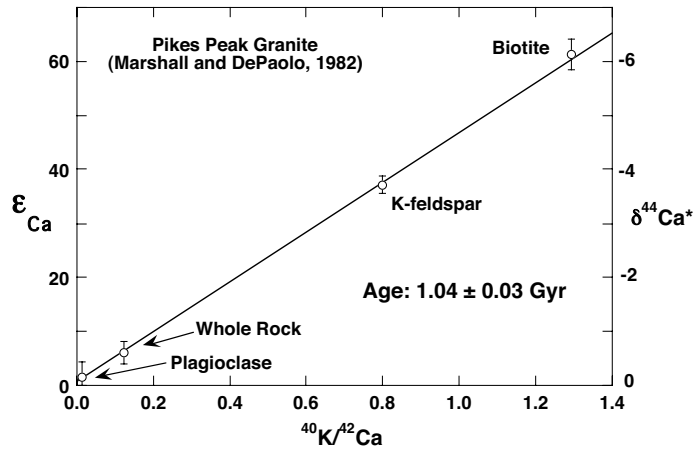
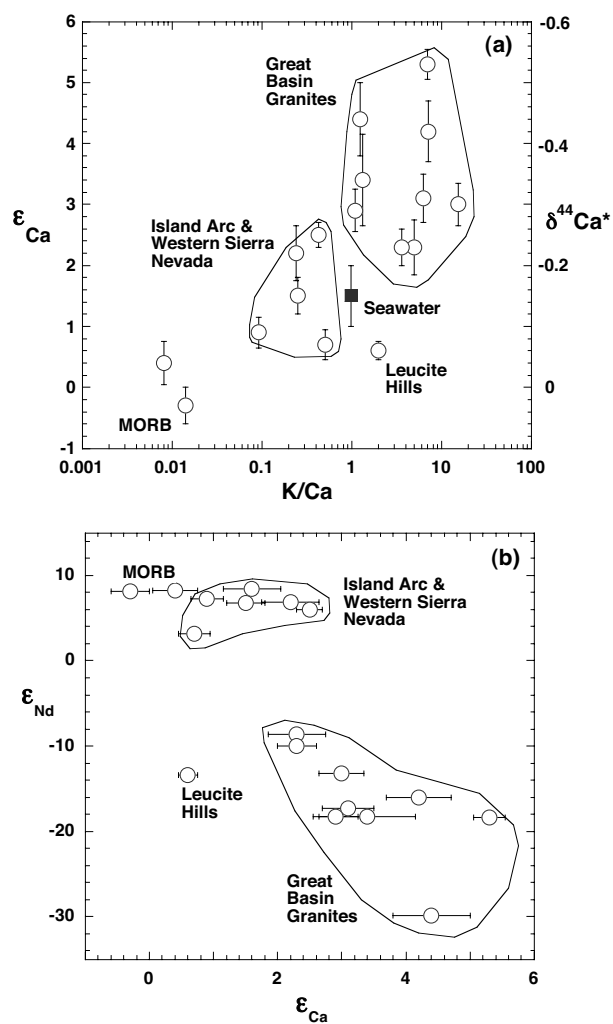


Figure 3. Variation of the $^{40}\text{Ca}/^{42}\text{Ca}$ value in minerals of the 1 billion year old Pikes Peak granite as measured by Marshall and DePaolo (1982). The currently accepted age is 1.08 Ga (Schärer and Allègre 1982; Smith et al. 1999). The left side scale shows the values as deviations from the mantle $^{40}\text{Ca}/^{42}\text{Ca}$ in units of ϵ_{Ca} , which is the parameter used to describe the radiogenic enrichments. The right side scale shows the equivalent value of $\delta^{44}\text{Ca}$ that would be inferred for a sample with radiogenic enrichment of ^{40}Ca , but analyzed according to the normal procedures for measuring mass dependent fractionation without correction for the radiogenic component. Whole rock ^{40}Ca enrichments typically are not greater than a few tenths of a unit of $\delta^{44}\text{Ca}$, but mineral ^{40}Ca enrichments can be quite large.

Figure 4. Radiogenic ^{40}Ca enrichments measured on whole rocks as reported by Marshall and DePaolo (1989), shown here as ϵ_{Ca} values with 1-sigma uncertainties and plotted versus (a) K/Ca and (b) ϵ_{Nd} value. The inferred value for seawater is also plotted in (a). Mid-ocean ridge basalts have no measurable enrichment of $^{40}\text{Ca}/^{42}\text{Ca}$ relative to the initial value for the Earth (151.016), as expected for magma derived from the Earth's mantle. Many granitic rocks, especially those with high K contents and low ϵ_{Nd} values, have significantly elevated ϵ_{Ca} values.



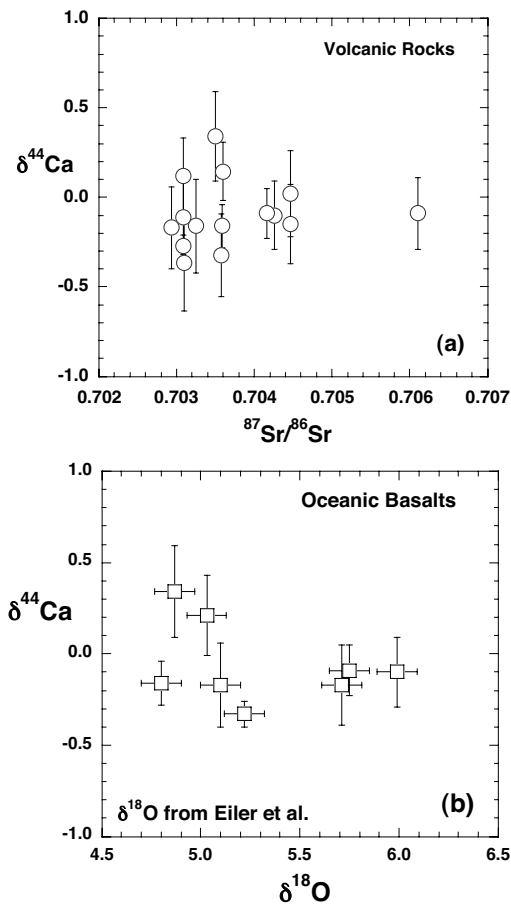


Figure 5. Available data on $\delta^{44}\text{Ca}$ values in oceanic basalts (Table 2) plotted against (a) $^{87}\text{Sr}/^{86}\text{Sr}$ and (b) $\delta^{18}\text{O}$. The average $\delta^{44}\text{Ca}$ value for all igneous rocks measured so far is -0.05 ± 0.2 . Small variations in mantle-derived igneous rocks could be expected as a result of recycling (subduction) of seawater-altered rocks, which would have relatively high $\delta^{44}\text{Ca}$, recycling of weathering products such as clay-rich sediment, which are also expected to have high $\delta^{44}\text{Ca}$ (not confirmed by measurements), recycling of oceanic carbonates, which have relatively low $\delta^{44}\text{Ca}$, and recycling of materials enriched in radiogenic ^{40}Ca .

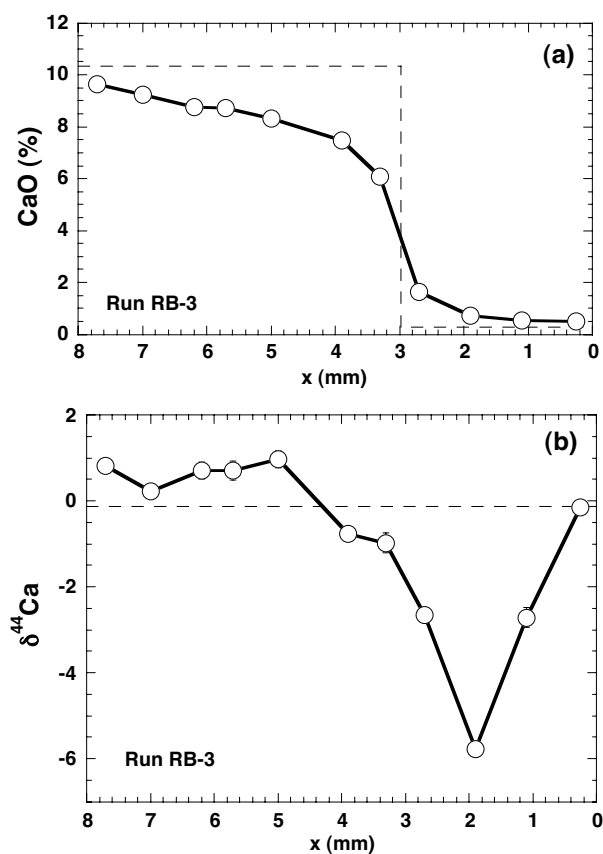


Figure 6. Results of a basalt-rhyolite liquid-liquid diffusion couple reported by Richter et al. (2003). The top figure shows the initial CaO concentration profile as a dashed line, and the final concentration profile as measured by electron microprobe. The lower figure shows the initial profile of $\delta^{44}\text{Ca}$ as a dashed line (the basalt value is -0.24 ± 0.05 and the rhyolite value -0.23 ± 0.05 , so they are identical) and the final values as measured on the run products. The ca. 6.5‰ variation was generated by preferential diffusion of light Ca isotopes from the basalt to the rhyolite during the run.

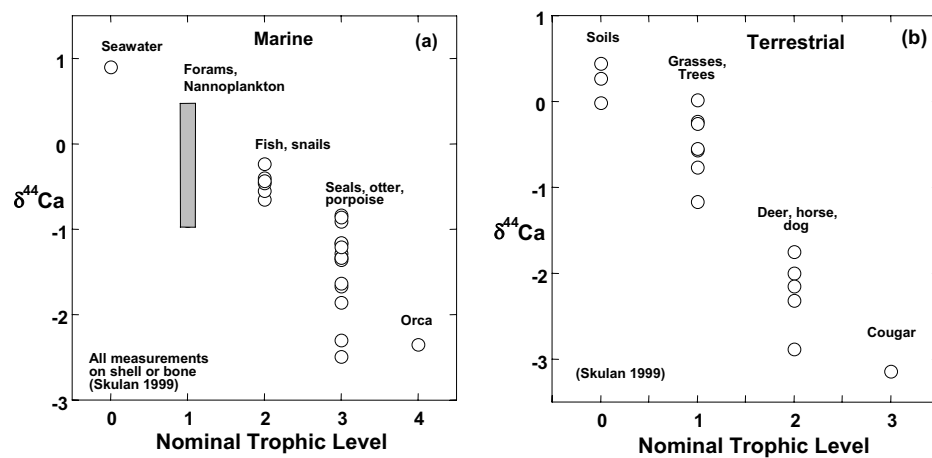


Figure 7. Summary of data suggesting that Ca isotopes are fractionated as calcium proceeds through food chains. Data are from Skulan et al. (1997), Skulan and DePaolo (1999) and Skulan (1999). Additional data are reported by Clementz et al. (2003).

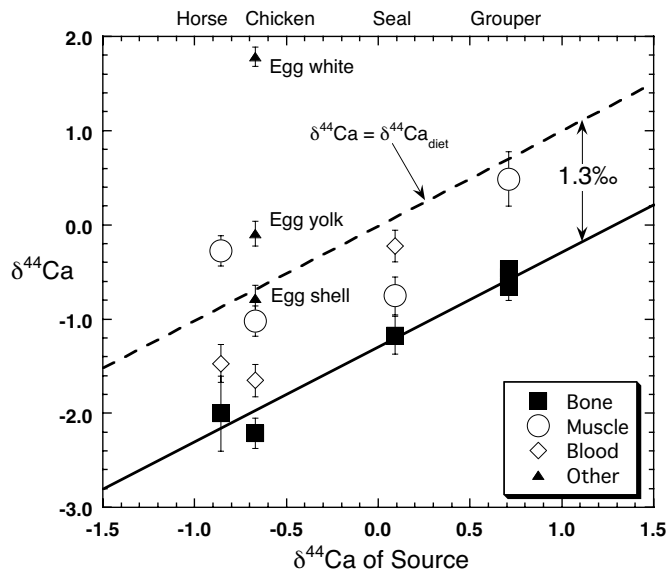
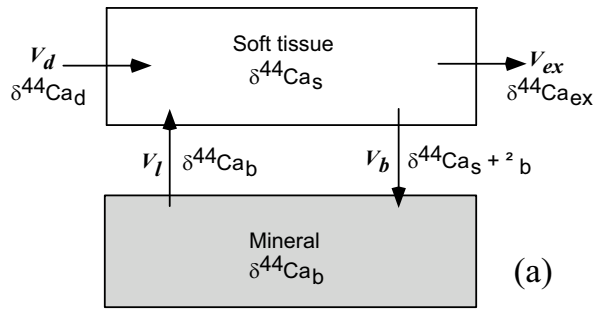
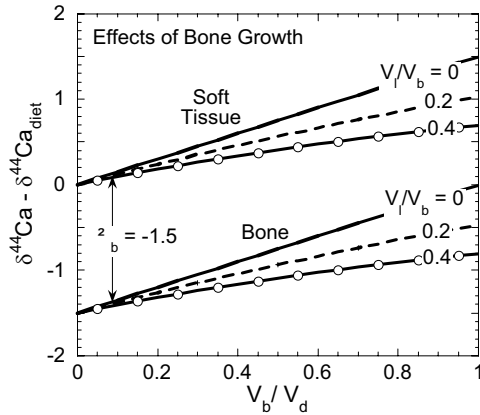


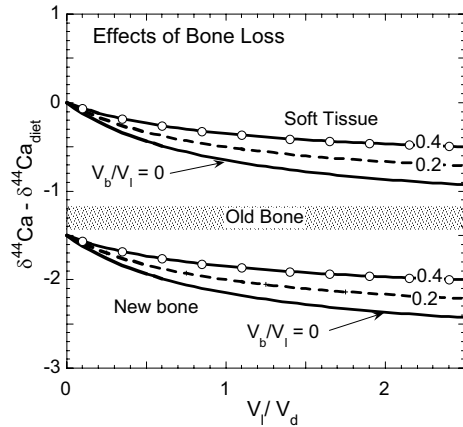
Figure 8. Calcium $\delta^{44}\text{Ca}$ values in vertebrate bone and soft tissue samples versus $\delta^{44}\text{Ca}$ in dietary source (Skulan and DePaolo 1999). Bone values are systematically about 1.3‰ lower than source values. Soft tissue values are more variable. All of the values are hypothesized to reflect the balance between Ca dietary intake and exchange with bone calcium (Fig. 9). The soft tissue values are variable largely because the residence time of Ca in the tissues is short. The high value of the egg white reflects Rayleigh-type distillation; the egg white loses light Ca to the shell as the shell forms. The small amount of Ca left in the egg white is highly fractionated. The low $\delta^{44}\text{Ca}$ value of the seal muscle is interpreted as a sign of distress; the seal may have had a dietary Ca deficiency for several days or longer before it died, and hence was deriving most of its Ca from bone dissolution.



(a)



(b)



(c)

Figure 9. (a) Box model of Skulan and DePaolo (1999) used to explain the $\delta^{44}\text{Ca}$ variations found in the bone and soft tissue of vertebrates. The $\delta^{44}\text{Ca}$ values of bone and soft tissue are generally determined by the ratios of the dietary Ca flux (V_d), to the Ca fluxes due to bone formation (V_b), and bone dissolution or loss (V_l). It is hypothesized that only the step associated with bone growth involves isotopic fractionation ($1000\ln\alpha = z_b = -1.5$). (b) Calculated effects on calcium isotopic fractionation due to variations of the ratio V_b/V_d , and (c) variations of the ratio V_l/V_d . In both cases, three curves are shown to describe the simultaneous variation of the third flux. Under healthy growth conditions, $V_b/V_d \ll 1$, and bone develops with $\delta^{44}\text{Ca}$ that is about 1.3‰ lower than the average value of the dietary calcium. When soft tissue Ca is heavily influenced by Ca derived from bone dissolution, then the soft tissue $\delta^{44}\text{Ca}$ values approach those of the average bone, and remodeled bone tends to be exceptionally low in $\delta^{44}\text{Ca}$.

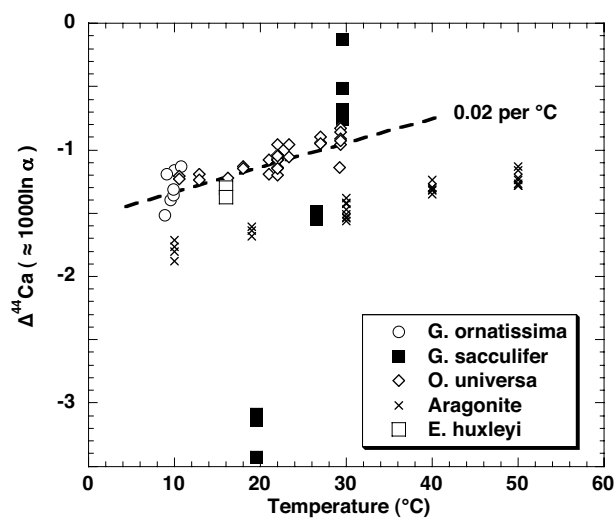


Figure 10. Summary of experimentally determined fractionation factors for Ca isotopes in the formation of foraminifera and coccolith shell carbonate, and for rapid inorganic precipitation of aragonite from an Mg-Ca-Cl solution. Data for the foraminifer *G. ornatissima* and the coccolith *E. huxleyi* are from DelaRocha and DePaolo (2000). Data on *G. sacculifer* are from Nagler et al. (2000). Data for *O. universa* and aragonite are from Gussone et al. (2003). Two of the forams and the coccolith *E. huxleyi* have similar fractionation behavior, with an overall fractionation factor of -1 to -1.5‰ , and a small temperature dependence of about 0.02 per $^{\circ}\text{C}$. The foram *G. sacculifer* appears to have a strongly temperature dependent fractionation factor.

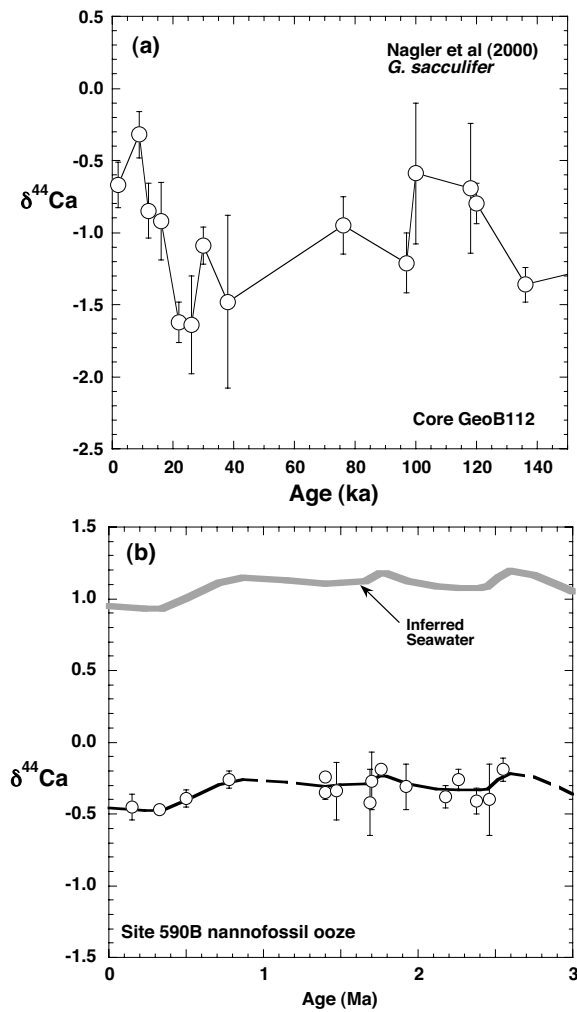


Figure 11. (a) Late Pleistocene $\delta^{44}\text{Ca}$ record based on measurements of *G. sacculifer* (from Nagler et al. 2000). The inferred variations of temperature are similar to those inferred from variations of Mg/Ca in the same sediment core. (b) Plio-Pleistocene record of seawater $\delta^{44}\text{Ca}$ based on bulk coccolith ooze from DSDP Site 590B in the southwestern Pacific (Tasman Sea). The 2.5 m.y. record shows only small variations of $\delta^{44}\text{Ca}$. The seawater curve is constructed assuming that the fractionation between seawater and bulk sediment remained constant. The decrease of $\delta^{44}\text{Ca}$ at ca. 0.7 Ma could reflect cooling rather than a change in the seawater $\delta^{44}\text{Ca}$.

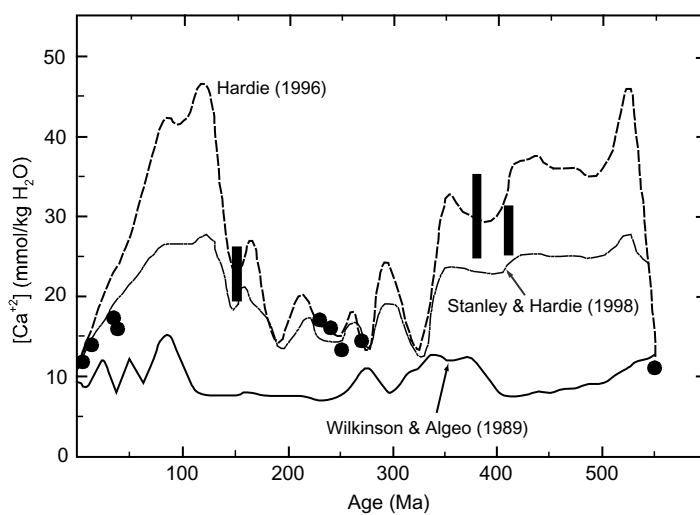


Figure 12. Models and data showing variations in the concentration of Ca^{2+} in the oceans over Phanerozoic time. Figure adapted from Horita et al. (2002), who used the mineralogy of evaporite deposits to infer the values shown as filled circles and bars.

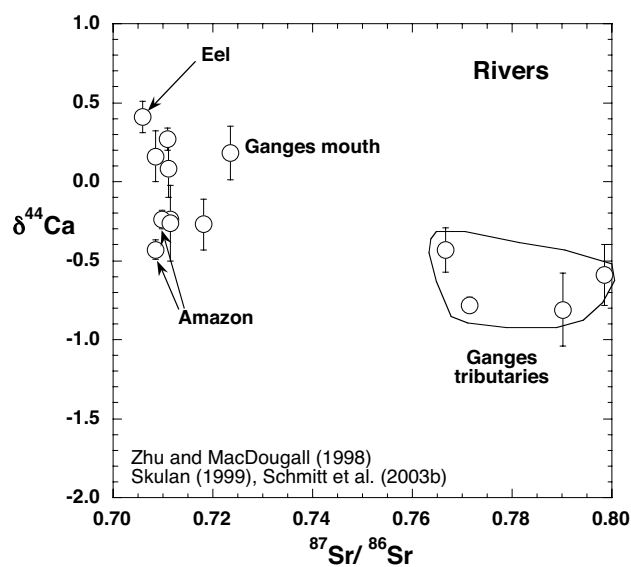


Figure 13. Variations of $\delta^{44}\text{Ca}$ and $^{87}\text{Sr}/^{86}\text{Sr}$ of dissolved Ca and Sr in rivers. There is variation of $>1.0\%$ in $\delta^{44}\text{Ca}$ although recently reported data (Schmitt et al. 2003) suggest that the low Ganges tributary values are not seen in samples from near the mouth of the Ganges.

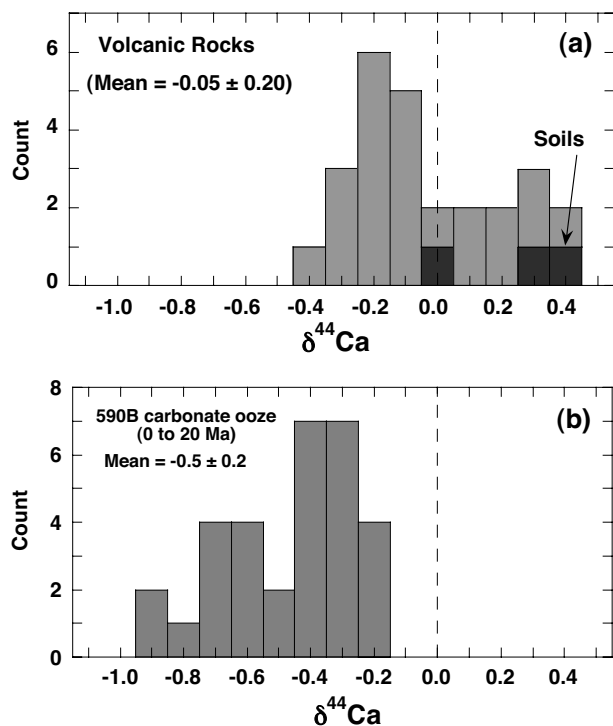


Figure 14. (a) Histogram of $\delta^{44}\text{Ca}$ values for volcanic rocks and for soils (data from Skulan et al. 1997; Skulan 1999; Zhu and MacDougall 1998; and Table 2). The average value of $\delta^{44}\text{Ca}$ is close to zero. Soils tend to have relatively high $\delta^{44}\text{Ca}$ suggesting that weathering preferentially removes light calcium isotopes. The average value of $\delta^{44}\text{Ca}$ in carbonate ooze from DSDP Site 590B is significantly lower than the average volcanic rock value, and similar to the average carbonate value reported by DelaRocha and DePaolo (2000). The data suggest that $\delta^{44}\text{Ca}$ of the overall weathering flux is lower than that of typical volcanic rocks.

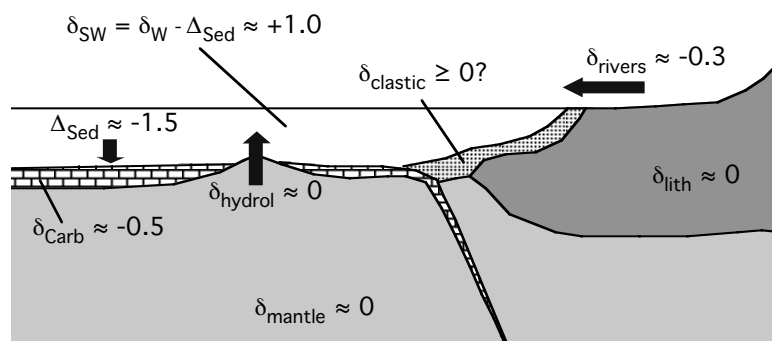


Figure 15. Diagram showing the major components of the global calcium cycle with $\delta^{44}\text{Ca}$ values (denoted as δ). The modern residence time of Ca in the oceans is about 1 million years (Holland 1978; 1984). Abbreviations used are: SW = seawater, Sed = sedimentation, clastic = clastic sediments, carb = marine carbonate sediments, hydrol = mid-ocean ridge hydrothermal systems, lith = continental lithosphere.

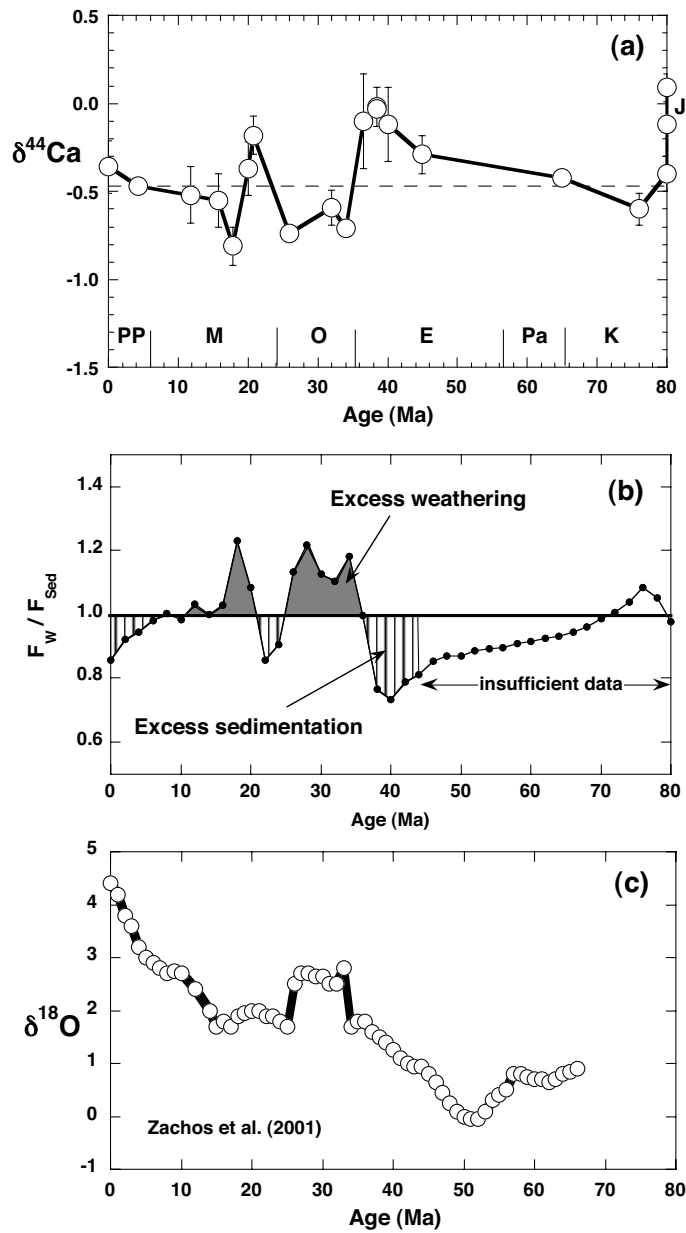


Figure 16. (a) Ca isotope record from marine carbonates (DelaRocha and DePaolo 2000). The variations are inferred to reflect variations in the isotopic composition of seawater (which is heavier by about 1.4‰). The small excursions of $\delta^{44}\text{Ca}$ reflect changes in the global weathering cycle; they are recast in (b) in terms of the ratio of the flux of calcium being delivered to the ocean by weathering (F_w) to the flux of Ca being removed from the ocean by carbonate sedimentation (F_{sed}). (c) Smoothed record of benthic foraminiferal $\delta^{18}\text{O}$ for the Cenozoic time period from Zachos et al. (2001)

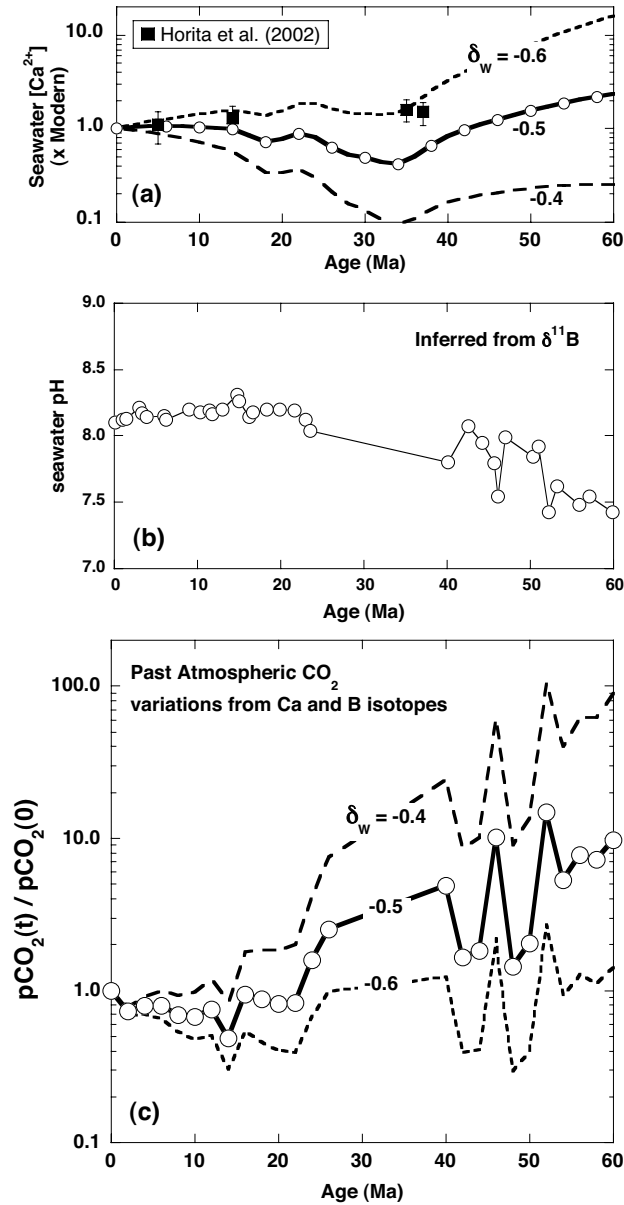


Figure 17. (a) Seawater calcium concentration versus geologic age calculated by integration of the F_w/F_{Sed} curve from Figure 16b under the assumptions that the residence time of Ca in seawater is constant and equal to 2 million years, and the $\delta^{44}Ca$ of the weathering flux is -0.5 ± 0.1 . The results are highly sensitive to the choice of the value of $\delta^{44}Ca$ for the riverine input and become more uncertain at greater age. Also shown are estimates of paleo-seawater $[Ca^{2+}]$ from Horita et al (2002) based on studies of fluid inclusions in evaporite minerals. (b) Inferred variation of ocean pH with geologic age based on the results of boron isotopic studies (Pearson and Palmer 2000). (c) Calculated atmospheric CO_2 concentration as function of geologic age using the curves from (a) and (b) and Equation (13). The value of $\log K$ is assumed to be constant.